INTELLECTUAL PROPERTY INDIA
PATENTS | DESIGNS | TRADE MARKS
GEOGRAPHICAL INDICATIONS

सत्यमेव जयते

क्रमांक : 044125823
SL No :

भारत सरकार
GOVERNMENT OF INDIA
पेटेंट कार्यालय
THE PATENT OFFICE

पेटेंट प्रमाणपत्र
PATENT CERTIFICATE

(Rule 74 Of The Patents Rules)

पेटेंट सं. / Patent No.	:	355248
आवेदन सं. / Application No.	:	201741037349
फाइल करने की तारीख / Date of Filing	:	23/10/2017
पेटेंटी / Patentee	:	INDIAN INSTITUTE OF TECHNOLOGY MADRAS (IIT Madras)

प्रमाणित किया जाता है कि पेटेंटी को उपरोक्त आवेदन में यथाप्रकटित METHOD OF MAKING NANOPARTICLES OF PRECISE ISOTOPIC COMPOSITION BY RAPID ISOTOPIC EXCHANGE नामक आविष्कार के लिए, पेटेंट अधिनियम, १९७० के उपबंधों के अनुसार आज तारीख 23rd day of October 2017 से बीस वर्ष की अवधि के लिए पेटेंट अनुदत्त किया गया है।

It is hereby certified that a patent has been granted to the patentee for an invention entitled METHOD OF MAKING NANOPARTICLES OF PRECISE ISOTOPIC COMPOSITION BY RAPID ISOTOPIC EXCHANGE as disclosed in the above mentioned application for the term of 20 years from the 23rd day of October 2017 in accordance with the provisions of the Patents Act,1970.

एकस्य कार्यालय THE PATENT OFFICE GOVT.OF INDIA भारत सरकार

अनुदान की तारीख : 04/01/2021
Date of Grant :

पेटेंट नियंत्रक
Controller of Patent

टिप्पणी - इस पेटेंट के नवीकरण के लिए फीस, यदि इसे बनाए रखा जाना है, **23rd day of October 2019** को और उसके पश्चात प्रत्येक वर्ष मे उसी दिन देय होगी।

Note. - The fees for renewal of this patent, if it is to be maintained will fall / has fallen due on 23rd day of October 2019 and on the same day in every year thereafter.

FORM 2

THE PATENTS ACT, 1970

(39 OF 1970)

&

The Patents Rules, 2003

COMPLETE SPECIFICATION

(Refer section 10 and rule 13)

TITLE OF THE INVENTION:

METHOD OF MAKING NANOPARTICLES OF PRECISE ISOTOPIC COMPOSITION BY RAPID ISOTOPIC EXCHANGE

2. APPLICANT:

(A) NAME: **INDIAN INSTITUTE OF TECHNOLOGY MADRAS (IIT Madras)**

(B) NATIONALITY: Indian

(C) ADDRESS:**INDIAN INSTITUTE OF TECHNOLOGY MADRAS**

IIT P.O

Chennai - 600 036

3. Preamble to the Description

COMPLETE SPECIFICATION

The following specification particularly describes the invention and the manner in which is to be performed.

COMPLETE SPECIFICATION

TITLE OF THE INVENTION

METHOD OF MAKING NANOPARTICLES OF PRECISE ISOTOPIC COMPOSITION BY RAPID ISOTOPIC EXCHANGE

FIELD OF THE INVENTION

The present invention relates to a method of making ligand protected nanoparticles of metal clusters of precise isotopic compositionby rapid and spontaneous isotopic exchange. The rapid exchange of the isotopes of the metal atoms helps to understand the mechanisms of the spontaneous structural changes in the nanoparticles.

BACKGROUND OF THE INVENTION

Since the discovery of deuterium (D) (H. C. Urey,*et al*., *Phys. Rev*. **1932**, *39*, 164-165) and the isolation of D_2O (G. N. Lewis, *et al.*, *J. Chem. Phys.,***1933**, *1*, 341-344), isotopic exchange in molecules has served as a characteristic signature of their dynamic chemical bonds (A. Thibblin, *et al.*, *Chem. Soc. Rev.,***1989**, *18*, 209-224). The rate of isotopic exchange in water ($H_2O + D_2O = 2HDO$) is fast with an equilibrium constant of 3.75±0.07 at room temperature (J. W. Pyper, *et al*., *J. Chem. Phys.,***1967**, *46*, 2253-2257) and it occurs at measurable speeds down to cryogenic temperatures (S.-C. Park, *et al*., *J. Chem. Phys.,***2004**, 121, 2765-2774). H/D exchange in proteins has been an important tool to understand their surface structure (L. Konermann, *et al*., *Chem. Soc. Rev.,***2011**, *40*, 1224-1234). Moreover, isotopic exchange in systems like H_2/D_2 has high activation barrier and occurs at very high temperatures (˜1000 K) or over heated catalytic metal surfaces (G. Pratt, *et al., J. Chem. Soc., Faraday Trans.,***1976**, *172*, 1589-1600). The existence of nanomaterials of noble metals with precise compositionallows the feasibility of their isotopic exchange to be tested.

Atomically precise noble metal clusters (I. Chakraborty,*et al.*,*Chem. Rev.***2017,***117*, 8208-8271,R.Jin,*et al., Chem. Rev.***2016,***116*, 10346-10413,A.Mathew, *et al*.,*Part. Part. Syst. Char.***2014,***31*, 1017-1053) are an interesting class of materials because of their structure and remarkable changes in properties compared to their bulk phases. Despite being structurally rigid and stabilized by a variety of protecting ligands like thiols and phosphines, theincreased

reactivityat the nanoscale is manifested in their spontaneous chemical reactions. Noble metal clusters like $Au_{25}(SR)_{18}$ (M. Zhu*, et al*.,*J. Am. Chem. Soc.* **2008,** *130*, 5883-5885) and $Ag_{44}(SR)_{30}$ (H. Yang,*et al., Nat Commun.* **2013,** *4*, 2422) undergo chemical reactions in solution under ambient conditions by spontaneous exchange of the metal atoms and the thiolate ligands (K.R. Krishnadas, *et al,. J. Am. Chem. Soc.* **2016**, *138*, 140-148). Similar reactivity is also observed between two structurally similar nanoclusters, $Au_{25}(SR)_{18}$ and $Ag_{25}(SR)_{18}$ (K. R. Krishnadas, *et al.Nat. Commun.* **2016**, *7*, 13447). For example, application number 6907/CHE/2015 illustrates a method of designing alloys of precise composition using such inter-cluster reactions in solution. Another application no. 201641034921 shows several aspects of mechanism of the inter-cluster reactions including the detection of reactive intermediates. However, complete understanding of such phenomenon is still unexplored.

Using high resolution electrospray ionization mass spectrometry (HR ESI MS), the present invention shows that atomically precise monolayer protected nanoclusters, made of isotopically pure silver (^{107}Ag and ^{109}Ag), despite their well-defined structures and ligand protection, undergo rapid exchange of the isotopes of the metal atoms. The exchange approaches a dynamic equilibrium within a minute in solution at room temperature. Using two archetypal examples of Ag nanoparticles of precise composition, $[Ag_{25}(SR)_{18}]$- (C. P. Joshi,*et al*., *J. Am. Chem. Soc.*, **2015**, *137*, 11578-11581) and $[Ag_{29}(S_2R)_{12}(TPP)_4]^{3-}$ (L. G. Abdul Halim, *et al*., *J. Am. Chem. Soc*. **2015**, *137*, 11970-11975) where SR, S_2R and TPP are protecting ligands, the invention demonstrate that the rapid isotopic exchange reflects their solution state dynamics. In addition, this shows the ability to control the exchange dynamics by controlling the temperature. Time resolved measurements further reveal that the mechanism of exchange involves several processes that occur at different timescales. The spontaneity in such reactions is mainly driven by the mixing entropy contribution to the free energy. Such an exchange mechanism, reminiscent of isotopic exchange between H_2O and D_2O, presents intriguing insights into the nature of nanoscale matter.

SUMMARY OF THE INVENTION

The present invention relates to atomically precise monolayer protected nanoparticles, made of isotopically pure silver which undergo rapid and spontaneous exchange of isotopes of Ag atoms, within a time scale of seconds, producing an equilibrium distribution. The rapid

exchange of the isotopes of the metal atoms helps to understand the mechanisms of the spontaneous structural changes in the clusters.

In one embodiment,the present invention relates to atomically precise silver cluster,$Ag_{25}(DMBT)_{18}$(C. P. Joshi, *et al. J. Am. Chem. Soc.* **2015,***137*, 11578-1158), where DMBT refers to 2,4-dimethyl benzene thiol. Isotopically pure clusters,$^{107}Ag_{25}(DMBT)_{18}$ and $^{109}Ag_{25}(DMBT)_{18}$ were prepared using isotopically pure $^{107}AgNO_3$ and $^{109}AgNO_3$ salts as the precursor for silver and following the same protocol for synthesizing the normal $Ag_{25}(DMBT)_{18}$ clusters. Isotopically pure samples, $^{107}Ag_{25}(DMBT)_{18}$ (m/z 5141) and $^{109}Ag_{25}(DMBT)_{18}$ (m/z 5191) shows identical optical absorption spectra. The isotopically pure samples were characterized by ESI MS which shows a separation of m/z 50 between their peak maxima.

In another embodiment, the invention shows the rate of exchange of the isotopes under ambient conditions was so fast that no intermediates were detected, the mixture reached the equilibrium situation instantly. Such rapid exchanges reflect the spontaneity of the chemical transformations and the high rates of interchanges in the structure. The mechanism of exchange must involve spontaneous breakage and reformation of Ag-Ag and Ag-S bonds, retaining the inherent structure of the cluster during the exchange. The rate of exchange of the isotopes of Ag atoms is also much faster compared to the rate of exchange with other metals like Ag-Au exchanges observed previously in the intercluster reactions.

BRIEF DESCRIPTION OF THE DRAWINGS

Figure 1 Mass spectra of the parent isotope clusters and the product of mixing.(A) ESI MS of the as-synthesized isotopically pure clusters, (a) $[^{107}Ag_{25}(DMBT)_{18}]^-$ and (b) $[^{109}Ag_{25}(DMBT)_{18}]^-$. (B) Mass spectral distribution of the product obtained by mixing the two isotopic clusters at 1:1 molar ratio. The spectrum was collected within 1 min after mixing the solutions of the clusters at room temperature.

Figure 2 Characterization of isotopically pure $[^{107}Ag_{25}(DMBT)_{18}]^-$ and $[^{109}Ag_{25}(DMBT)_{18}]^-$ clusters.(A) UV-vis spectra of $[^{107}Ag_{25}(DMBT)_{18}]^-$ and $[^{109}Ag_{25}(DMBT)_{18}]^-$ clusters showing identical features. ESI MS of (B) $[Ag_{25}(DMBT)_{18}]^-$ made from natural Ag, (C) $[^{107}Ag_{25}(DMBT)_{18}]^-$ and (D) $[^{109}Ag_{25}(DMBT)_{18}]^-$. Insets show the comparison of the experimental and calculated isotope patterns of the peaks. The minor differences in the

experimental spectra (in C and D) in comparison to the calculated spectra are due to the slight contribution of the other isotope in each sample as the isotope enrichment was 98%.

Figure 3 Isotope patterns of the product obtained by reaction of $[^{107}Ag_{25}(DMBT)_{18}]^-$ and $[^{109}Ag_{25}(DMBT)_{18}]^-$ at 1:1 molar ratio. Experimental isotope distribution of the product obtained by mixing $[^{107}Ag_{25}(DMBT)_{18}]^-$ and $[^{109}Ag_{25}(DMBT)_{18}]^-$ at 1:1 molar ratio. The isotope pattern is compared with (A) the distribution computed considering 50% abundance of each isotope in $[Ag_{25}(DMBT)_{18}]^-$ and (B) experimental isotope patterns of $[Ag_{25}(DMBT)_{18}]^-$ synthesized from natural Ag.

Figure 4 ESI MS of reaction product obtained by mixing the two isotopic $[^{107}Ag_{25}(DMBT)_{18}]^-$ and $[^{109}Ag_{25}(DMBT)_{18}]^-$ clusters at various molar ratios. Product obtained by mixing $[^{107}Ag_{25}(DMBT)_{18}]^-$ and $[^{109}Ag_{25}(DMBT)_{18}]^-$ at varying molar ratios where in (A) $[^{107}Ag_{25}(DMBT)_{18}]^-$ cluster is kept in higher concentration and in (B) $[^{109}Ag_{25}(DMBT)_{18}]^-$ cluster is kept in higher concentration. The initial molar ratio of mixing the two clusters ($[^{107}Ag_{25}(DMBT)_{18}]^-$: $[^{109}Ag_{25}(DMBT)_{18}]^-$) is indicated for each product observed.

Figure 5 Comparison of the experimental and calculated isotope patterns of the products obtained by mixing $[^{107}Ag_{25}(DMBT)_{18}]^-$ and $[^{109}Ag_{25}(DMBT)_{18}]^-$ at various molar ratios. Comparison of the experimental isotope patterns of the products obtained at different molar ratios of mixing the two isotopic clusters ($[^{107}Ag_{25}(DMBT)_{18}]^-$:$[^{109}Ag_{25}(DMBT)_{18}]^-$) with the calculated patterns. The experimental patterns showed best match with the calculated patterns considering the abundances of each isotope in the cluster from their initial molar ratio of mixing.

Figure 6 Low temperature reactions showing the intermediate steps of exchange. Exchange between the two isotopic $[Ag_{25}(DMBT)_{18}]^-$ clusters at -20 ^oC showing the intermediate stages of exchange (a)-(d) with mixing time (s). Distributions (i) and (ii) denote exchange at the $[^{107}Ag_{25}(DMBT)_{18}]^-$ and $[^{109}Ag_{25}(DMBT)_{18}]^-$ sides, respectively. Noise in the spectrum is due to the short acquisition time.

Figure7 Isotope exchange in$[Ag_{24}Au(DMBT)_{18}]^-$clusters. ESI MS of (A) $[^{107}Ag_{24}Au(DMBT)_{18}]$- and (B) $[^{109}Ag_{24}Au(DMBT)_{18}]^-$. Insets show the comparison of the experimental and calculated isotope patterns. (C) Reaction of $[^{107}Ag_{24}Au(DMBT)_{18}]$- and $[^{109}\ Ag_{24}Au\ (DMBT)_{18}]^-$ in 1:1 molar ratio at room temperature, where (i), (ii) and (iii) denotes ESI MS of

$[^{107}Ag_{24}Au(DMBT)_{18}]^-$, $[^{109}Ag_{24}Au(DMBT)_{18}]^-$ and the product (50% abundance of each isotope), respectively. All the spectra are shown in the same scale.(D) Intermediates stages of reaction in 1:1 molar ratio at -20°C.(E)and(F) Reaction at various molar ratios, $[^{107}Ag_{24}Au(DMBT)_{18}]^-$: $[^{109}Ag_{24}Au(DMBT)_{18}]^-$ ratio is indicated in the figure.

Figure 8 Characterization of isotopically pure $[^{107}Ag_{29}(BDT)_{12}(TPP)_4]^{3-}$ and $[^{109}Ag_{29}(BDT)_{12}(TPP)_4]^{3-}$ clusters. ESI MS of (A) $[^{107}Ag_{29}(BDT)_{12}]^{3-}$ and (B) $[^{109}Ag_{29}(BDT)_{12}]^{3-}$ clusters. The labile TPP ligands were lost during ionization. Insets show the comparison of the experimental and calculated isotope patterns of the peaks. The minor differences in the experimental spectra in comparison to the calculated spectra are due to the slight contribution of the other isotope in each sample as the isotope enrichment was 98%. (C), UV-vis spectra of $[^{107}Ag_{29}(BDT)_{12}(TPP)_4]^{3-}$ and $[^{109}Ag_{29}(BDT)_{12}(TPP)_4]^{3-}$ clusters showing identical features.

Figure 9 Reaction between $[^{107}Ag_{29}(BDT)_{12}]^{3-}$ and $[^{109}Ag_{29}(BDT)_{12}]^{3-}$ clusters in 1:1 molar ratio at room temperature. (A) Intermediates stages of reaction between $[^{107}Ag_{29}(BDT)_{12}]^{3-}$ and $[^{109}Ag_{29}(BDT)_{12}]^{3-}$ in 1:1 molar ratio at room temperature. The mixture reaches equilibrium over a period of 2 h. (B) Intermediates stages of reaction between $[^{107}Ag_{29}(BDT)_{12}(TPP)_n]^{3-}$ (n=0-4) and $[^{109}Ag_{29}(BDT)_{12}(TPP)_n]^{3-}$ (n=0-4) in 1:1 molar ratio at room temperature, showing the intact TPP attached clusters in ESI MS. The mixture reaches equilibrium at similar time scales.

Figure 10 ESI MS of reaction product obtained by mixing the two isotopic $[^{107}Ag_{29}(BDT)_{12}(TPP)_4]^{3-}$ and $[^{109}Ag_{29}(BDT)_{12}(TPP)_4]^{3-}$ clusters at various molar ratios.(A) Product obtained by mixing the two isotopic clusters $[^{107}Ag_{29}(BDT)_{12}]^{3-}$ and $[^{109}Ag_{29}(BDT)_{12}]^{3-}$ at varying molar ratios where in (a) $[^{107}Ag_{29}(BDT)_{12}]^{3-}$ is kept in higher concentration and in (b) $[^{109}Ag_{29}(BDT)_{12}]^{3-}$ is kept in higher concentration. The initial molar ratio of mixing the two clusters ($[^{107}Ag_{29}(BDT)_{12}]^{3-}$: $[^{109}Ag_{29}(BDT)_{12}]^{3-}$) is indicated for each product observed. (B) Comparison of the experimental isotope patterns of the products with the calculated isotope patterns considering the abundances of each isotope from their initial molar ratio of mixing.

Figure 11 Kinetic study of isotopic exchange in $[Ag_{29}(BDT)_{12}(TPP)_4]^{3-}$ clusters. Plot of percentage of un-exchanged parent isotopic cluster (C_t) vs time (min) at room temperature (25°C). Kinetics at 40°C and 60°C are presented in the inset. Average of three kinetic measurements is plotted and the error bar is indicated at each point. A schematic showing the

different stages of isotopic exchange is also shown in the figure. Color codes: yellow: S, orange: P, transparent grey: ligands.

Figure 12 Time dependent study of reaction between $[^{107}Ag_{29}(BDT)_{12}]^{3-}$ and $[^{109}Ag_{29}(BDT)_{12}]^{3-}$ in 1:1 molar ratio at various temperatures. Time-dependent study showing the intermediates stages of reaction between $[^{107}Ag_{29}(BDT)_{12}]^{3-}$ and $[^{109}Ag_{29}(BDT)_{12}]^{3-}$ in 1:1 molar ratio at (A) 40^oC, (B) 60 ^oC and (C) 0^oC.(D) Kinetic plot of the percentage of un-exchanged parent cluster (C_t) versus time at 0^oC. The rate constants obtained from tri-exponential fitting are indicated in the figure.

Figure 13 Kinetic study of the isotopic exchange in $[Ag_{29}(BDT)_{12}(TPP)_4]^{3-}$ clusters at 1:1 molar ratio at different concentrations of the parent cluster. Time-dependent ESI MS and corresponding kinetic study showing the rate constants of the reaction at A) $1.5*10^{-5}$mM and B) $1.5*10^{-1}$mM concentration.

Figure 14 Kinetic study of isotopic exchange in $[Ag_{29}(BDT)_{12}(TPP)_4]^{3-}$ clusters ($1.5*10^{-3}$mM concentration of parent clusters) at different molar ratios of mixing. Kinetic study of isotopic exchange at molar ratios of mixing of $^{107}Ag_{29}$:$^{109}Ag_{29}$ clusters, (A) 2.5:1 and (B) 5:1. The rate constants of the three stages of exchange in each case are denoted in the figure.

Figure 15 Time dependent study of reaction between $[^{107}Ag_{29}(BDT)_{12}]^{3-}$ and $[^{109}Ag_{29}(BDT)_{12}]^{3-}$ ($1.5*10^{-3}$mM concentration of parent clusters) at various molar ratios. Time-dependent study showing the intermediate stages of reaction at $^{107}Ag_{29}$:$^{109}Ag_{29}$ molar ratios of (A) 2.5:1 and (B) 5:1.

Figure 16 Molecular docking studies. Force-field global minimum geometry (FFGMG) of two (A) $[Ag_{25}(DMBT)_{18}]^-$ and (B) $[Ag_{29}(BDT)_{12}(TPP)_4]^{3-}$ clusters, lying in close-proximity. Color codes: grey: Ag, yellow: S, orange: P, the overlapping Borromean rings are shown in blue, green and red in (A), staple units are shown in green and blue in (B), and ligand shell is shown in transparent grey. Atomic diameters have been reduced to show the bonding clearly.

Figure 17 Molecular docking studies. Lowest energy geometry obtained from docking two A) $Ag_{25}(DMBT)_{18}$ and B) $Ag_{29}(BDT)_{12}(TPP)_4$ clusters. C-H…π interactions are indicated in the figure. Color codes: grey: Ag, yellow: S, orange: P, green: ligands. The H atoms involved in

these interactions are shown in red and the benzene rings involved are shown in blue. Expanded view of the ligands involved in these C-H…π interactions are shown in the insets b.

Referring to the drawings, the embodiments of the present invention are further described. The figures are not necessarily drawn to scale, and in some instances the drawings have been exaggerated or simplified for illustrative purposes only. One of ordinary skill in the art may appreciate the many possible applications and variations of the present invention based on the following examples of possible embodiments of the present invention.

DETAILED DESCRIPTION OF THE INVENTION

The following description is presented to enable any person skilled in the art to make and use the embodiments, and is provided in the context of a particular application and its requirements. Various modifications to the disclosed embodiments will be readily apparent to those skilled in the art, and the general principles defined herein may be applied to other embodiments and applications without departing from the spirit and scope of the present disclosure. Thus, the present invention is not limited to the embodiments shown, but is to be accorded the widest scope consistent with the principles and features disclosed herein.

The present invention relates to an atomically precise monolayer protected nanoparticle, made of isotopically pure silver which undergo rapid exchange of isotopes of Ag atoms, within a time scale of seconds, producing an equilibrium distribution. The rapid exchange of the isotopes of the metal atoms helps to understand the mechanisms of the spontaneous structural changes in the clusters.

The present invention shows a spontaneous isotopic exchange occur between atomically precise silver nanoclusters. While it is rapid in $[Ag_{25}(SR)_{18}]^-$, it is relatively slower in $[Ag_{29}(S_2R)_{12}(TPP)_4]^{3-}$, reflecting the differences in their chemical structures. Spontaneity in such reactions, driven by their entropy of mixing, reflects the dynamic nature of nanoparticles in solution. However, the invention is restricted only to sub-nanometer sized clusters, where exchange is shown to be dependent on their inherent structures. In a similar manner, it may also be extended to classic nanomaterials of various sizes.

The present invention illustrates an experiment with a well known atomically precise silver cluster,$Ag_{25}(DMBT)_{18}$, where DMBT refers to 2,4-dimethyl benzene thiol. The structure of the cluster is known from single crystal X-ray diffraction (C. P. Joshi, *et al. J. Am. Chem. Soc.*

2015,*137*, 11578-1158). Isotopically pure (98%) metal samples, ^{107}Ag and ^{109}Ag, were purchased from Cambridge Isotopes Laboratories. $AgNO_3$ was prepared from the isotopically pure metal foils.The isotopically pure metal foils were reacted with hot nitric acid (70 %) which resulted in the formation of silver nitrate, water, and oxides of nitrogen.Fine crystals of the isotopically pure $AgNO_3$salt were recrystallized from water. Isotopically pure clusters, $^{107}Ag_{25}(DMBT)_{18}$ and $^{109}Ag_{25}(DMBT)_{18}$ were prepared using isotopically pure $^{107}AgNO_3$ and $^{109}AgNO_3$ salts as the precursor for silver and following the same protocol for synthesizing the normal $Ag_{25}(DMBT)_{18}$ clusters (C. P. Joshi, *et al. J. Am. Chem. Soc.* **2015,***137*, 11578-11581).In a typical synthesis, about 38 mg of $^{107}AgNO_3$or$^{109}AgNO_3$was dissolved in a mixture of 2 mL methanol and 17 mL DCM and 90 μL of 2,4-dimethyl benzene thiol (2,4-DMBT) was added to it to form a yellow insoluble Ag-S complex and the mixture was kept under stirring condition at 0^oC. After about 15-17 min, 6 mg of PPh_4Br in 0.5 mL of methanol was added. This was followed by the dropwise addition of a solution of 15 mg of $NaBH_4$ in 0.5 mL of ice-cold water. The reaction mixture was kept under stirring condition for about 7-8 h. After that, stirring was discontinued and the solution was kept at 4 ^oC for about 2 days. For purification of the cluster, the sample was centrifuged to remove any insoluble impurities and DCM was removed by rotary evaporation. The precipitate was washed twice with methanol. After that, the cluster was redissolved in DCM and again centrifuged to remove any further insoluble contaminants. DCM was removed finally by rotary evaporation and thus the purified clusters were obtained in powder form.

For isotopic exchange, $[Ag_{25}(SR)_{18}]^-$ clusters (C. P. Joshi, *et al. J. Am. Chem. Soc.* **2015,** *137*, 11578-11581) were chosen initially. Two identical but isotopically different clusters, $[^{107}Ag_{25}(DMBT)_{18}]^-$ and $[^{109}Ag_{25}(DMBT)_{18}]^-$ (DMBT is 2,4-dimethyl benzene thiol), were prepared starting from isotopically pure metals and extensively characterized to ensure their chemical purity and isotopic identity. The isotopic clusters showed identical optical absorption spectra (Fig. 2A). ESI MS of $[^{107}Ag_{25}(SR)_{18}]^-$ and $[^{109}Ag_{25}(SR)_{18}]^-$are presented in Fig. 1A (a) and (b), respectively. The peak maxima of the spectra are separated by m/z 50, due to the interchange of 25 atoms of ^{107}Ag with ^{109}Ag. The mass spectral distributions of the isotopic clusters are narrower than that of a sample with natural Ag (Fig. 2B). The isotope patterns (Fig. 2C, D) are purely due to the isotopes of S, C and H in the ligands and therefore, it is similar to that of $[Au_{25}(PET)_{18}]^-$ cluster (M. Zhu,*et al.*, *J. Am. Chem. Soc*, **2008**, *130*, 5883-5885; M. W. Heaven, *et al.*, *J. Am. Chem. Soc*. **2008**, *130*, 3754-3755) (PET is phenyl ethane thiol, PET has

the same atomic composition ($C_8H_{10}S$) as DMBT), as Au has only one isotope. The minor differences with calculated patterns (Fig. 2C, D) are due to the slight isotopic impurity as the isotope enrichment was ~98%. Upon mixing an equimolar mixture of $[^{107}Ag_{25}(DMBT)_{18}]^-$ and $[^{109}Ag_{25}(DMBT)_{18}]^-$ in solution at room temperature, the spectrum changed instantaneously and the resulting distribution is shown in Fig. 1B. No peaks due to the parent clusters were observed indicating that they were totally exchanged in this process. The mass spectral distribution calculated (Fig. 3A) considering a system where each isotope of Ag (107/109) has a probability of occupying 50% of the total sites of the cluster is similar to the distribution observed in Fig. 1B. It is nearly identical to that of the ion $[Ag_{25}(DMBT)_{18}]^-$, having the natural isotope distribution (^{107}Ag: 51.839%, ^{109}Ag: 48.161%), and the minor differences arise as ^{107}Ag:^{109}Ag ratio is not exactly 1:1 in nature (Fig. 3B). The two isotopically pure clusters were further mixed at varying molar ratios and in each case rapid exchange between the two clusters resulted in a binomial mass spectral distribution (Fig. 4), in agreement with the calculated isotope pattern considering the relative abundance of each isotope from their initial molar ratio of mixing (Fig. 5). Such an equilibrium statistical distribution is expected for a system where there are nearly equivalent sites which have equal probability of exchange.

Control over the exchange dynamics was achieved by lowering the temperature. The parent solutions were cooled to -20^{o}C, mixed in 1:1 molar ratio and ESI MS was measured instantly. The source and desolvation temperatures were lowered to 30^{o}C and the sample was infused from an external syringe which was also cooled to -20^{o}C in order to reduce the effect of temperature during injection. In Fig. 6a-d, we presented the intermediate stages involving stepwise exchange of the isotopes of the atoms between the two clusters. Although the reaction kinetics was slower at lower temperatures, the equilibrium distribution was attained in about 30 s. Rapid exchange occurred even in alloys of the cluster *(*M. S. Bootharaju, *et al., Angew. Chem. Int. Ed*. **2016**, *55*, 922-926), as similar observations were made in the case of $[Ag_{24}Au(SR)_{18}]^-$ (Fig. 7).

In order to probe the dynamics of the exchange process controlled by the inherent structures of the cluster, a similar experiment is performed with $[Ag_{29}(BDT)_{12}(TPP)_4]^{3-}$, where the dithiolate protection provides a very different structure *(*L. G. AbdulHalim, *et al., J. Am. Chem. Soc.***2015**, *137*, 11970-11975) as compared to that of $[Ag_{25}(DMBT)_{18}]^-$. Isotopically pure $[^{107}Ag_{29}(BDT)_{12}(TPP)_4]^{3-}$ and $[^{109}Ag_{29}(BDT)_{12}(TPP)_4]^{3-}$ clusters were synthesized and

characterized using optical absorption (Fig. 8C) and ESI MS (Fig. 8A, B). A reduced exchange rate was observed compared to that of $[Ag_{25}(DMBT)_{18}]^-$. At room temperature, an equimolar mixture of the two isotopic $[Ag_{29}(BDT)_{12}(TPP)_4]^{3-}$ clusters,at a concentration of $1.5*10^{-3}$mM, showed stepwise exchanges reaching a dynamic equilibrium over a period of 3 h (Fig. 9A). Though the labile TPP ligands were lost during ionization, the use of soft ionization conditions enabled us to observe that exchange occurred at similar rate to that in the intact TPP protected clusters that exist in solution (Fig. 9B). The clusters mixed at any arbitrary molar ratios also attained equilibrium in a similar manner and in all cases the relative abundance of the isotopes in the final product was in accordance with their initial molar ratio of mixing (Fig. 10).

The slower exchange rates seen here encouraged us to analyze the dynamics in greater detail. A kinetic plot of the percentage of un-exchanged parent isotopic cluster (C_t) versus time (t) is shown in Fig. 11. At a particular time, the percentage of exchange on either of the two isotopic clusters was similar when mixed in equimolar quantities. Therefore, monitoring the kinetics with respect to either of them gave identical results. A hypothetical data point at t = 0 min, C_t = 100%, assuming that at 0 min, i.e. in an ideal situation before mixing, the abundance of a particular isotope ($^{107}Ag/^{109}Ag$) in the clusters is 100%. Fig. 11 shows that at room temperature (25 ^oC), the $^{107}Ag/^{109}Ag$ exchange rate was initially fast and within 8-10 min, about 30% exchange had occurred. Later, the exchange progressed slowly and after about 300 min, the rate slowed down further, approaching an equilibrium corresponding to a state of 50% exchange. A tri-exponential effectively fitted the data points suggesting at least three different rates for the exchange process with rate constants of $5.9*10^{-1}$ min^{-1}, $1.4*10^{-2}$ $min^{-1}$and $7.1*10^{-18}$ min^{-1}, respectively. Similar exchange was studied at higher temperatures of 40 ^oC and 60 ^oC (Fig. 12A, B) and the kinetic plots are shown in the inset of Fig. 11. The rate increased significantly at higher temperatures and the reaction was complete within 60 min, whereas upon cooling the reaction mixture to 0 ^oC, the rate was drastically reduced and the process took around 3 days to attain equilibrium (Fig. 12C, D). Similar features were also observed for H/D exchange in supramolecular polymers in water (X. Lou,*et al.*, *Nat. Commun*. **2017**, 8, 15420). The three stages of exchange suggest that possibly the isotopic exchange in nanoparticles proceeds through i) rapid exchange of their surface atoms, ii) slower diffusion of the exchanged atoms within the core and iii) subsequent equilibration in the whole cluster. The reaction rates were dependent on

the concentration of the clusters, which was evident from the kinetic studies in case of a significantly lower ($1.5*10^{-5}$mM) and higher ($1.5*10^{-1}$mM) concentration of theparent clusters compared to the above case ($1.5*10^{-3}$mM) (Fig. 13).At a particular concentration of the parent clusters, we have also investigated the reaction rates in case of the reactions at different molar ratios of mixing. Keeping the total number of moles of the mixture as constant, and starting from an excess concentration of $[^{107}Ag_{29}(BDT)_{12}(TPP)_4]^{3-}$, the rate increases with an increase in the concentration of $[^{109}Ag_{29}(BDT)_{12}(TPP)_4]^{3-}$, reaching a maximum at 1:1 condition. As the relative concentration of $[^{109}Ag_{29}(BDT)_{12}(TPP)_4]^{3-}$ in the reaction mixture increases, the number of effective collisions between the isotopically different entities increases and hence the rate of exchange increases. Similar results were obtained starting from an excess concentration of $[^{109}Ag_{29}(BDT)_{12}(TPP)_4]^{3-}$and slowly increasing the concentration of $[^{107}Ag_{29}(BDT)_{12}(TPP)_4]^{3-}$ in the mixture. Kinetic studies at different molar ratios showing the rate constants (Fig. 14), and corresponding time-dependent ESI MS (Fig. 15) are included in the supplementary information.Moreover, the reaction rates were similar in different solvents like DMF/ACN/DCM etc.

Mechanism and the driving forces of the isotopic exchange reaction were demonstrated by molecular docking studies and free energy calculations. The mechanism of atom exchange is expected to be initiated through inter-cluster collisions (K. R. Krishnadas,*et al.*, *Nat. Commun.* **2016**, 7, 13447), and this is consistent with the temperature dependence of the rate constants. Molecular docking simulations was carried out for studying the interaction between two $[Ag_{25}(DMBT)_{18}]^-$and two $[Ag_{29}(BDT)_{12}(TPP)_4]^{3-}$ clusters. In each case, docking generated ten different possible orientations and the lowest energy geometries for the approach of two $[Ag_{25}(DMBT)_{18}]^-$ and two $[Ag_{29}(BDT)_{12}(TPP)_4]^{3-}$clusters are represented in Fig. 16A and 16B, respectively. However, the other possible geometries were also similar in both cases where the two clusters approach along the same orientation or along other symmetry equivalent orientations such that they interact at similar sites and generate the same configuration. The other possibilities are also energetically similar within0.01-0.07 kcal/mol. As all the possible structures obtained from docking are geometrically and energetically equivalent, it is likely that exchange reaction will be more favorable when the clusters approach along this specific geometry. The force-field global minimum geometry (FFGMG) obtained by docking two $[Ag_{25}(DMBT)_{18}]^-$

clusters indicates thatpost-collision, the clusters may bind together supramolecularly in the initial steps of the reaction with an interaction energy of -23.7 kcal/mol between the two clusters (Fig. 16A). The rapid exchange and the structural changes in $[Ag_{25}(DMBT)_{18}]^-$ can also be viewed from their topologically simplified structure (referred to as the aspicule model) which considers the structure of a $M_{25}L_{18}$ cluster (where M = Au,Ag; L=ligand) as a system of three interlocked Borromean rings of $M_8(SR)_6$ around a central M atom. Rapid exchange of isolobal$Ag_2(SR)_3$ and $Ag(SR)_2$ entities may occur. The opening of the rings can also make the core more exposed and facilitate spontaneous exchange of Ag or Ag-SR units between the core and staples of the two clusters. In comparison, $[Ag_{29}(BDT)_{12}(TPP)_4]^{3-}$ does not contain any interlocked rings or chain structures. It has a rigid surface network with cross-linking dithiolates in the outer shell. In the lowest energy geometry of two $[Ag_{29}(BDT)_{12}(TPP)_4]^{3-}$ clusters (Fig. 16B), the proximity of Ag_3S_6 or AgS_3P motifs of the two clusters may result in opening up of these staples. Molecular docking reveals an interaction energy of -7.8 kcal/mol between two $[Ag_{29}(BDT)_{12}(TPP)_4]^{3-}$ clusters (Fig. 16B). The supramolecular interactions between the clusters mainly include van der Waals and C-H$\cdots\pi$ interactions. In the case of $[Ag_{25}(DMBT)_{18}]^-$ clusters, the H of the benzene ring and $-CH_3$ group from one cluster can interact with the π-system of the benzene ring of DMBT ligand of another cluster to facilitate the binding. These C-H$\cdots\pi$ interaction distances are in the range of 2.99 to 4.16 Åwhich are comparable with the C-H$\cdots\pi$ distances observed in the crystal structures of $Au_{246}$and Ag_{29} nanoclusters. Interactions are similar in the case of $[Ag_{29}(BDT)_{12}(TPP)_4]^{3-}$ clusters also. The C-H$\cdots\pi$ interactions exist between –H of BDT of one cluster with benzene ring of BDT of another cluster at a distance of about 3.46 to 4.39 Å. The interactions are more in $[Ag_{25}(DMBT)_{18}]^-$ cluster and hence results in higher binding energy. The interactions between the ligands are indicated in Fig.17. The lesser inter-cluster interaction energy and higher rigidity in the structure of $[Ag_{29}(BDT)_{12}(TPP)_4]^{3-}$ might result in a slower exchange rate as compared to that of $[Ag_{25}(DMBT)_{18}]^-$. However, more detailed computations are required to understand the complete mechanism of the atom exchange process.

The thermodynamics of the reaction to identify the main driving force of the isotopic exchange reaction. The energy barrier for an inter-cluster isotopic exchange represents the energy cost of breaking and reforming bonds, and any intermediate barriers which must be crossed while the atoms travel along the path from their initial to final positions. We computed the enthalpic (electronic energy, zero-point energy (ZPE) and specific heat) and the entropic

(electronic, translational, rotational and vibrational) contributions to the free energy. Computational details are mentioned in the methods section and detailed results are presented in Table 1-4. The total electronic energies of the clusters do not vary when different isotopes of the atoms are exchanged and rearranged since their bonding interactions are identical. Hence, any differences in enthalpy will be due to ZPE. Furthermore, the vibrational contribution to enthalpy and entropy will also contribute to the free energy. However, we found that there were only very small differences in the free energy of the clusters (~ 0.01 eV) due to isotopic exchange, and moreover, these differences cancel out when the reaction free energy (ΔG_{react} = G(products)-G(reactants)) is computed for the 1:1 ratio. In this calculation, we have assumed the parent clusters are the isotopically pure reactants and the products are the two mixed isotope clusters with composition, (m,n) = (12,13) and (13,12) in the case of $[^{107}Ag_m{}^{109}Ag_n(DMBT)_{18}]^-$ and (m,n) = (14,15) and (15,14), in the case of $[^{107}Ag_m{}^{109}Ag_n(BDT)_{12}(TPP)_4]^{3-}$. Thus, in the absence of other contributions to the reaction free energy, the contribution from the mixing of isotopic clusters is expected to be of central importance in understanding the driving force of the reaction.

Application of the concept of entropy to a single cluster is not proper due to the small number of atoms (10^2–10^3) in an individual cluster, however, we may apply it to the macroscopically large ensemble of *N* clusters, and the ensemble configuration is defined by the positions of ^{107}Ag and ^{109}Ag atoms in *N* clusters, where *N* is taken to be in the thermodynamic limit. The final equilibrium state of the cluster ensemble will be that in which the number of isotopic substituent is maximum for a given molar ratio, so that the whole ensemble of clusters has the highest entropy (S) which is defined as S= *k*logW, where W is total the number of ways of arranging the two isotopes of Ag atoms (microstates) in the total available sites of the clusters and *k* is the Boltzmann constant. For the equimolar composition, this will occur for the half-mixed compositions of each clusters, *i.e*, *n* = (12, 13) and (13, 12) for Ag_{25} and (14, 15) or (15, 14) for Ag_{29}, where these compositions have the identical maximum degeneracy in positional arrangements.

Ensemble of clusters with two crystalline lattices consisting one of ^{107}Ag and another of ^{109}Ag are fused together and then assume random thermal exchanges of atoms in the joint lattice. In this simplification, only the Ag atoms were considered, neglecting the cluster structure and symmetry and all interatomic interactions, and this situation is identical to the mixing of two

ideal gases. Hence, the expression for mixing or configurational entropy is simply that of mixing two different ideal gases, which is known from statistical mechanics, and is given by,

$$\Delta S_{mix} = -n_{mol}R[p\ln p+(1-p)\ln(1-p)]$$

where p is the molefraction of ^{107}Ag, (1-p) is the mole fraction of ^{109}Ag and n_{mol} is the total number of moles of the mixture. ΔS_{mix} attains its maximum negative value for the half-and-half mixture i.e. p = 0.5, for a given total number of moles of the mixture. For a 1:1 ratio of mixing, ΔS_{mix} is $R\ln 2$ = 5.76 $JK^{-1}mol^{-1}$ which is 1.37 $calK^{-1}mol^{-1}$, and ΔG_{mix}= -T*ΔS_{mix}= -408.26 $calmol^{-1}$ (T = 298 K and n_{mol} = 1). Since, the calculated reaction free energies are negligible; the mixing entropic contribution to the free energy must be the main driving force of the spontaneous reaction as observed. We remark that the mixing entropy term would also be important in spontaneous bimetallic inter-cluster reactions where there are larger enthalpic changes due to the bonding interactions such as those between $Ag_{25}(DMBT)_{18}$ and $Au_{25}(PET)_{18}$.(K. R. Krishnadas, et al., *Nat. Commun.***2016**, *7*, 13447)

The following description explains the experimental method of synthesis of isotopically pure clusters and its reaction;-

Synthesis of isotopically pure silver nitrate ($^{107}AgNO_3$ and $^{109}AgNO_3$) from isotopically pure metal foils (^{107}Ag and ^{109}Ag)

About 50 mg of the metal foils of the isotopes of Ag (^{107}Ag and ^{109}Ag) was separately reacted with about 2 mL concentrated nitric acid (70 %) in a 5 mL reaction vessel and heated at 70 ^{o}C inside a fumehood. The heating was continued until the evolution of nitrogen oxide gases was complete and the solution turned colorless. The solution was then diluted with water and heating was continued. The process of addition of water was continued for a few times and finally a concentrated solution of about 0.5 mL of $AgNO_3$ was kept for crystallization. For crystallization, the solution was kept inside an airtight dark box in presence of solid P_2O_5 and NaOH pellets (kept separately in the same box) to enhance the evaporation of water and remove excess acid respectively. Colorless crystals of $AgNO_3$ were obtained within 5-7 days. The yield of the reaction was around 95%.

Synthesis of isotopically pure $[^{107}Ag_{25}(DMBT)_{18}]^-[PPh_4]^+$ and $[^{109}Ag_{25}(DMBT)_{18}]^-[PPh_4]^+$ clusters

Isotopically pure clusters were synthesized using the isotopically pure $AgNO_3$ salt which was synthesized according to the above mentioned method. The clusters were synthesized following a reported protocol(C. P. Joshi, *et al. J. Am. Chem. Soc.* **2015,***137*, 11578-1158). About 38 mg of $^{107}AgNO_3/^{107}AgNO_3$ was dissolved in a mixture of 2 mL methanol and 17 mL DCM. To this reaction mixture, about 90 µL of 2,4-DMBT was added. The mixture was kept under stirring condition at 0 ^oC. About 6 mg of PPh_4Br in 0.5 mL of methanol was added after about 15-20 min. Next, about 15 mg of $NaBH_4$ in 0.5 mL of ice-cold water was added to the solution in a dropwise fashion. The stirring was continued for about 7-8 h and then the solution was stored at 4 ^oC for about 2 days. For purification, the sample was centrifuged and DCM was removed by rotary evaporation. The precipitate was washed twice with methanol. Then the cluster was redissolved in DCM and centrifuged to remove any further insoluble impurities. Further removal of DCM by rotary evaporation led to the formation of the purified clusters ($[^{107}Ag_{25}(DMBT)_{18}]^-[PPh_4]^+$ /$[^{109}Ag_{25}(DMBT)_{18}]^-$ $[PPh_4]^+$) in their powder form.

Synthesis of isotopically pure $[^{107}Ag_{29}(BDT)_{12}(TPP)_4]^{3-}$and $[^{107}Ag_{29}(BDT)_{12}(TPP)_4]^{3-}$clusters

Isotopically pure clusters were synthesized using the isotopically pure $AgNO_3$ salt following a reported method*(*L. G. AbdulHalim, *et al., J. Am. Chem. Soc.***2015**, *137*, 11970-11975). About 20 mg of $^{107}AgNO_3/^{109}AgNO_3$ was dissolved in a mixture of 5 mL MeOH and 10 mL DCM. To this solution, about 13.5 µl of 1,3-BDT ligand was added and the reaction mixture was kept under stirring condition. Addition of the thiol immediately resulted in a turbid yellow solution which turned clear upon addition of about 200 mg of PPh_3. After about 15 min, a freshly prepared solution of 10.5 mg of $NaBH_4$ in 500 µl of water was added. The stirring was continued under dark conditions for 3-5 h. During the course of the reaction, the dark brown color of the solution changed to orange. After completion of the reaction, the mixture was centrifuged and the supernatant was discarded. The precipitate consisting of Ag_{29} cluster was washed repeatedly with methanol. The sample was dissolved in DMF and again centrifuged to remove any further insoluble contaminants. The supernatant was vacuum dried and the purified clusters ($[^{107}Ag_{29}(BDT)_{12}(TPP)_4]^{3-}$/$[^{107}Ag_{29}(BDT)_{12}(TPP)_4]^{3-}$) were obtained in the powder form.

Synthesis of isotopically pure $[^{107}Ag_{24}Au(DMBT)_{18}]^-$ and $[^{109}Ag_{24}Au(DMBT)_{18}]^-$ clusters

Isotopically pure $[^{107}Ag_{25}(DMBT)_{18}]^-$ and $[^{109}Ag_{25}(DMBT)_{18}]^-$ clusters were used as the precursor to which Au^+ was added in a controlled manner such that galvanic replacement of a Ag

atom with Au resulted in the formation of $[^{107}Ag_{24}Au(DMBT)_{18}]^-$ and $[^{109}Ag_{24}Au(DMBT)_{18}]^-$ clusters (M. W. Heaven, *et al.*, *J. Am. Chem. Soc*. **2008**, *130*,3754-3755),respectively.

Reaction of the isotopically pure clusters

Stock solutions of parent isotopically pure clusters were prepared at a concentration of $1.5*10^{-3}$mM, in each case. Then they were mixed in different molar ratios and their reaction was monitored by ESI MS.

Instrumentation

The optical absorption spectra were measured in PerkinElmer Lambda 25 UV-vis spectrophotometer. All the mass spectrometric measurements were done in a Waters Synapt G2 Si instrument. The instrument is well equipped with electrospray ionization (ESI) and all spectra were measured in the negative ion and resolution mode. The instrument is capable of measuring ESI MS with high resolution touching orders of 50,000 (m/Δm). The instrument was calibrated using NaI. An optimized condition involving capillary voltage: 3 kV, cone voltage: 20 V, desolvation gas flow: 400 L/h, source temperature: 100 ^oC, desolvation temperature: 150 ^oC, sample infusion rate: 30μL/h was used for all measurements. For low temperature measurements the source and desolvation temperatures were lowered to 30 ^oC, and the sample was infused by an external syringe which was also cooled at -20 ^oC.

Computational Methods

Free energy calculations

The exchange effect of silver isotopes (^{107}Ag and ^{109}Ag) was computationally studied in $[Ag_{25}(DMBT)_{18}]$- and $[Ag_{29}(BDT)_{12}(PPh_3)_4]^{3-}$ clusters by calculating free energy and thermo-chemistry parameters such as zero-point energy (ZPE), enthalpy (H) and entropy (S) using density functional theory (DFT) as implemented in real-space grid based projector augmented wave (GPAW) package(J. J. Mortensen*, et al*., *Phys. Rev. B*, **2005**, *71*, 035109). The PAW setup $Ag(4d^{10}5s^1)$, $S(3s^23p^4)$, $P(3s^23p^3)$, $C(2s^22p^2)$ and $H(1s^1)$ was considered to include only the valence electronic structure for the constituent atoms including the scalar-relativistic effects for Ag. Further, a reduced model was used considering $-CH_3$ instead of the benzene rings in DMBT, BDT and TPP ligands, to reduce the high computational time of frequency calculations. The real space calculation in finite difference (FD) mode along with PBE functional was applied for the geometry optimizations with a grid spacing of 0.2 Å and the minimization criterion was the

residual forces of 0.05 eV/Å, without considering any symmetry constraints. The atomic masses of Ag isotopes were taken as 106.905 and 108.905 for ^{107}Ag and ^{109}Ag respectively. The vibrational modes were calculated only for Ag, S and P atoms using the finite difference approximation of the Hessian matrix by considering the two displacements (+ delta and - delta) per atom in each Cartesian coordinate. Further, the calculated vibrational energies were used to calculate the thermo-dynamic quantities like H, S and Gibbs free energy (G).

The calculation of G is made in the ideal gas approximation. It includes the electronic energy (E_{pot}), zero-point energy (E_{ZPE}), translational, rotational and vibrational components of H and S, which are based on DFT calculations. Additional entropy of mixing component was calculated separately from statistical mechanics.

Enthalpy (H) is calculated within the atomistic simulation environment, as

$H = E_{pot} + E_{ZPE} + C_{v\_trans} + C_{v\_rot} + C_{v\_vib,}$ and entropy is $S = S_{trans} + S_{rot} + S_{elec} + S_{vib}$

Hence, the Gibb's free energy at temperature 'T' and pressure 'P' is calculated as,

$G = H - T*S$

The structural isomers of each isotopically substituted cluster arising from the different possible ways of arranging *n* Ag isotopic substituent atoms among the total number of Ag atoms, are all degenerate as far as their total electronic energy is concerned with a small difference of only 0.01 eV for Ag_{29} and Ag_{25} in the value of G of the parent and isotopic substituent clusters in terms of their enthalpic and the vibrational entropic components (Table 1-4).

Table 1 showing zero-point energy (ZPE) and Gibbs free energy (G) values of the isotopic clusters $[Ag_{29}(BDT)_{12}(TPP)_4]^{3-}$ clusters (Isotopically pure reactants)

Cluster	**ZPE (eV)**	**G (eV)**
$[^{107}Ag_{29}(BDT)_{12}(TPP)_4]^{3-}$	2.400	-1262.250
$[^{109}Ag_{29}(BDT)_{12}(TPP)_4]^{3-}$	2.394	-1262.271

Table 2 Mixed isotope product clusters with composition (m,n)=(15,14) and (14,15) in $[^{107}Ag_m{}^{109}Ag_n(BDT)_{12}(TPP)_4]^{3-}$

(m.n) = (15,14)				(m.n) = (14,15)			
Position of ^{107}Ag atoms	**Position of ^{109}Ag atoms**	**ZPE (eV)**	**G (eV)**	**Position of ^{107}Ag atoms**	**Position of ^{109}Ag atoms**	**ZPE (eV)**	**G (eV)**
C-1 I-12 S-2	S-14	2.397	-1262.260	S-14	C-1 I-12 S-2	2.397	-1262.261
S-15	C-1 I-12 S-1	2.397	-1262.260	C-1 I-12 S-1	S-15	2.397	-1262.261
C-1 I-6 S-8	I-6 S-8	2.397	-1262.260	I-6 S-8	C-1 I-6 S-8	2.397	-1262.261

Table 3 showing zero-point energy (ZPE) and Gibbs free energy (G) values of the isotopic clusters $[Ag_{25}(DMBT)_{18}]^-$ clusters (Isotopically pure reactants)

Cluster	**Zero-point energy (ZPE) (eV)**	**Free Energy (G) (eV)**
$[^{107}Ag_{25}(DMBT)_{18}]^-$	1.655	-502.919
$[^{109}Ag_{25}(DMBT)_{18}]^-$	1.650	-502.938

Table 4 (Mixed isotope product clusters with composition (m,n)=(13,12) and (12,13) in $[^{107}Ag_m{}^{109}Ag_n(DMBT)_{18}]^-$

(m.n) = (13,12)				(m.n) = (12,13)			
Position of ^{107}Ag	**Position of ^{109}Ag**	**ZPE (eV)**	**G (eV)**	**Position of ^{107}Ag**	**Position of ^{109}Ag**	**ZPE (eV)**	**G (eV)**

atoms	atoms			atoms	atoms		
C-1 I-12	S-12	1.652	-502.928	S-12	C-1 I-12	1.652	-502.929
S-12 C/I-1	C/I-12	1.652	-502.928	C/I-12	S-12 C/I-1	1.652	-502.929
C-1 I-6 S-6	I-6 S-6	1.652	-502.928	I-6 S-6	C-1 I-6 S-6	1.652	-502.929

(N.B. C, I and S refers to centre, icosahedron and staple positions, respectively)

The reaction equations for the 1:1 ratio mixing as follows,

Wherein, (m,n) = (12,13) and (13,12) for Ag_{25} and (m,n) = (14,15) and (15,14) for Ag_{29} are equally likely to form.

$[^{107}Ag_{25}(DMBT)_{18}]^{-}+[^{109}Ag_{25}(DMBT)_{18}]^{-} \longrightarrow [^{107}Ag_{13}{}^{109}Ag_{12}(DMBT)_{18}]^{-}+ [^{107}Ag_{12}{}^{109}Ag_{13}(DMBT)_{18}]^{-}$

For the case of $[Ag_{29}(BDT)_{12}(TPP)_4]^{3-}$,

$[^{107}Ag_{29}(BDT)_{12}(TPP)_4]^{3-}+ [^{109}Ag_{29}(BDT)_{12}(TPP)_4]^{3-} \longrightarrow$

$[^{107}Ag_{15}{}^{109}Ag_{14}(BDT)_{12}(TPP)_4]^{3-} + [^{107}Ag_{14}{}^{109}Ag_{15}(BDT)_{12}(TPP)_4]^{3-}$

For (m,n) = (12,13), (13,12) in $[Ag_{25}(DMBT)_{18}]$- and (m,n) = (14,15), (15,14) in $[Ag_{29}(BDT)_{12}(TPP)_4]^{3-}$ substituent cases (1:1 molar ratio), we have computed the reaction molar Gibbs free energy (ΔG_{react}) at standard temperature (298 K) and pressure (1 atm). The reaction free energies (ΔG_{react}) are zero for both Ag_{29} and Ag_{25} clusters (Table1-4) and the overall free energy of reaction is given by,

$\Delta G = \Delta G_{react} + \Delta G_{mix} = G(products)-G(reactants) + \Delta G_{mix}$

For $[Ag_{25}(DMBT)_{18}]^{-}$,

G(products) = G of $^{107}Ag^{109}Ag$ (12,13)+ G of $^{107}Ag^{109}Ag$ (13,12)

G(reactants) = G of parent $^{107}Ag_{25}$ + G of parent $^{109}Ag_{25}$

and similarly for Ag_{29}.

The expression for mixing or configurational entropy is simply that of mixing two different ideal gases, which is known from statistical mechanics, and is given by,

$$\Delta S_{mix} = -n_{mol}R[(p\ln p + (1-p)\ln(1-p)]$$

where p is the molefraction of ^{107}Ag, $(1-p)$ is the mole fraction of ^{109}Ag and n_{mol} is the total number of moles of the mixture. We note that the mixing entropy is independent of the cluster size and only depends on the mixing ratio, hence, we expect the half-and-half-mixture to have the largest mixing free energy. For the 1:1 mixture we have $p = 0.5$, and hence term is ΔS_{mix} is $R\ln 2$ ($n_{mol} = 1$) and $\Delta G_{mix} = -T*\Delta S_{mix} = -RT\ln 2$, where R is the gas constant in Jmol^{-1}, and $n_{mol} = 1$. This analysis reveals that the entropy of isotopic mixing is the largest and most significant contribution to the Gibbs free energy. Due to the fractional mixing ratio, the mixing entropy is always positive, and therefore $\Delta G_{mix}$is always negative and is larger than the other terms in the free energy. Hence, ΔG_{mix}, being the largest contribution to the overall reaction causes ΔG always to be negative which makes the reaction spontaneous.

The mixing ratio $x = 0.5$, corresponds to the nearest integer numbers of exchanged Ag atoms to half of total number of Ag atoms in the cluster, since both clusters have an odd number of Ag atoms, *eg*. (25/2) = 12.5, hence, (13,12) or (12,13) where these compositions both have the identical maximum degeneracy in arrangements as a function of the number of substituents n in Ag_{25} cluster. Similarly, for Ag_{29} cluster, (29/2) = 14.5 and hence, (14,15) or (15,14) are the most entropically favourable compositions in Ag_{29}.

Molecular Docking

In order to understand the inter-molecular interactions in $[Ag_{25}(SR)_{18}]^-$ clusters, molecular docking studies were performed using AutoDock4.2 and its associated tools(G. M. Morris.*et al.*, *J. Comput. Chem*. **2009**, *30*, 2785-2791). DFT optimized geometry and partial charges of $[Ag_{25}(SR)_{18}]^-$ were used for this study. $[Ag_{25}(SR)_{18}]^-$was used as both 'ligand' and 'receptor'. Receptor grids were generated using 126 × 126 × 126 grid points in xyz with grid spacing of 0.375 Å and map types were created using AutoGrid-4.2. The grid parameter file (.gpf) was saved using MGL Tools-1.4.6.50. The docking parameter files (.dpf) were generated using MGLTools-1.4.6.50. The results of AutoDock generated an output file (.dlg), and the generated conformers were scored and ranked as per the interaction energy. Ten lowest energy conformers were obtained. Lamarckian genetic algorithm was used for the output file using

MGLTools-1.4.6. The binding free energy of the force-field global minimum geometry (FFGMG) of the dimeric cluster adduct was -23.7 kcal/mol. Similar study was done with $[Ag_{29}(S_2R)_{12}(TPP)_4]^{3-}$ clusters, where $[Ag_{29}(S_2R)_{12}(TPP)_4]^{3-}$ was used as both ligand and receptor. In this case, the binding free energy of FFGMG of the dimeric adduct was -7.8 kcal/mol.

Calculation of theoretical isotope patterns with varying composition of ^{107}Ag/^{109}Ag: The theoretical isotope patterns of $[Ag_{25}(DMBT)_{18}]^-$ and $[Ag_{29}(BDT)_{12}(TPP)_4]^{3-}$ calculated by varying the abundance of each isotope (^{107}Ag/^{109}Ag) in them by 1% change so that the composition is (x,y) i.e., {(100,0), (99,1), (98,2).....(0,100)} where x and y are the abundance of ^{107}Ag and ^{109}Ag respectively. The experimental spectra were compared with the calculated spectra to find the best match and hence confirm the composition.

Details of fitting the kinetic data

The tri-exponential fitting in Figure 3 was performed using the Origin 8.5 software package. The equation $y = k_1\exp(-t*a) + k_2\exp(-t* b) + k_3\exp(-t*c)$ was used for the tri-exponential fits. The parameters k_1, k_2, k_3, a, b, c were varied during the fitting and t was used as the independent variable. Both mono-exponential and bi-exponential fits were inadequate and only a triexponential fit could successfully fit the data points.

Such rapid isotope exchanges are expected to occur for other protected silver nanoparticles like $[Ag_{44}(SR)_{30}]$(H. Yang, *et al*.,*Nat Commun***2013,***4*, 2422), $[Ag_{29}(S_2R)_{12}]$ (L. G. AbdulHalim, *et al.*, *J. Am. Chem. Soc.*, **2015**, *137*, 11970–11975), etc., as they all have the similar chemistry and also a range of alloy clusters like,$Ag_{25-x}Au_x(SR)_{18}$ can be created where the composition of Ag is selectively modified. The exchange is also expected for metal nanoparticles protected by different types of ligands like thiols, phosphines or amines. Moreover, apart from Ag, other metals like Pd, Pt, Ni, Cu etc., are rich in isotopes. Naturally occurring Pd is composed of six stable isotopes: ^{102}Pd,^{104}Pd, ^{105}Pd, ^{106}Pd, ^{108}Pd, and ^{110}Pd. Naturally occurring Pt is composed of five stable isotopes: ^{192}Pt, ^{194}Pt, ^{195}Pt, ^{196}Pt and ^{198}Pt. Similar exchange behavior is also expected for metal nanoparticles made of Pd, Pt, Ni, Cu etc. The physical properties of the clusters are expected to show changes upon isotopic substitution. Clusters with varying isotopic composition can be put on surfaces to create surfaces with different catalytic reactivity.Alloy

clusters containing more than one type of metal atom are also very important in terms of their catalytic and optical properties. A variety of doped alloy clusters have been reported in literature like $[MAg_{24}(SR)_{18}]^{2-}$ (M = Pd, Pt) (J. Yan, *et al.*, *J. Am. Chem. Soc.* **2015,** *137*, 11880-11883), $PtAg_{28}(BDT)_{12}(TPP)_4$(M. S. Bootharaju, *et al*. *Nanoscale* **2017,** *9*, 9529-9536), $[Pt_2Ag_{23}Cl_7(PPh_3)_{10}]$ (M. S. Bootharaju, *et al*., *J. Am. Chem. Soc.* **2017,** *139*, 1053-1056).In such alloy clusters, the isotopic composition of both the metals can be selectively modified andall of the above phenomenon can also happen with the alloy clusters composed of these metals.

It may be appreciated by those skilled in the art that the drawings, examples and detailed description herein are to be regarded in an illustrative rather than a restrictive manner.

We Claim: **CLEAN COPY**

1. A method for making isotopically pure ligand protected metal nanoparticles of precise isotopic composition by rapid and spontaneous isotopic exchange, the said method comprises;

   mixing isotopically pure nanoparticles of the same metal in different molar ratio, and controlled isotopic exchange of metal atoms between isotopically pure metallic nanoparticles by controlling the temperature in the range from -20°C to 60°C and concentration in the range from ~10^{-5}mM to ~10^{-1}mM

   wherein, the exchange of isotopic atoms is facilitated by the collision between the clusters and occurs due to the spontaneous transfer of metal atoms between the two clusters that is driven by the entropy of mixing of clusters.

2. The method as claimed in claim 1, wherein the isotopically pure metal is ^{107}Ag and ^{109}Ag.
3. The method as claimed in claim 1, wherein the ligand protected metallic nanoparticles include $Ag_{25}(SR)_{18}$, $Ag_{29}(S_2R)_{12}$, $Ag_{44}(SR)_{30}$, where SR is a thioland S_2R is a dithiol.
4. The method as claimed in claim 1, wherein the protecting ligand of the nanoparticles is selected from thiols, phosphines and amines.
5. The method as claimed in claim 3, wherein SR is a thiol group is selected from 2,4-dimethyl benzene thiol (DMBT) and S_2R is a dithiol group is selected from 1,3-benzene dithiol (BDT).
6. The method as claimed in claim 1, wherein the isotopically pure metal clusters are $[^{107}Ag_{25}(SR)_{18}]^-$, $[^{109}Ag_{25}(SR)_{18}]^-$, $[^{107}Ag_{29}(S_2R)_{12}(TPP)_4]^{3-}$ and $[^{109}Ag_{29}(S_2R)_{12}(TPP)_4]^3$, wherein SR is a thiol group, S_2R is a dithiol group, and TPP is triphenyl phosphine.
7. The method as claimed in claim 6, wherein the mixture of isotopically pure metal clusters $[^{107}Ag_{25}(DMBT)_{18}]^-$ and $[^{109}Ag_{25}(DMBT)_{18}]^-$in the ratio 1:1 rapidly exchange isotopes to form $[^{107}Ag_{12}{}^{109}Ag_{13}(DMBT)_{18}]^-$ and $[^{107}Ag_{13}{}^{109}Ag_{12}(DMBT)_{18}]^-$ clusters.
8. The method as claimed in claim 6, wherein the mixture of isotopically pure metal clusters $[^{107}Ag_{29}(BDT)_{12}(TPP)_4]^{3-}$ and $[^{109}Ag_{29}(BDT)_{12}(TPP)_4]^{3-}$ in the ratio 1:1 rapidly exchange isotopes to form $[^{107}Ag_{14}{}^{109}Ag_{15}(BDT)_{12}(TPP)_4]^{3-}$ and $[^{107}Ag_{15}{}^{109}Ag_{14}(BDT)_{12}(TPP)_4]^{3-}$ clusters.
9. The method as claimed in claim 2, wherein the isotopic atoms of Ag is selectively modified to make $Ag_{24}Au(SR)_{18}$ alloy cluster.
10. The method as claimed in claim 7, wherein specific atomic locations in alloy clusters are retained without exchange.

11. The method as claimed in claim 1, wherein the exchange effect of precise isotopic metal clusters is calculated by free energy and thermo-chemistry parameters including zero-point energy (ZPE), enthalpy (H) and entropy.

Dated at Chennai this August 04, 2020

Signature: 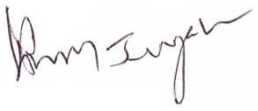

D. Moses Jeyakaran
Advocate & Patent Agent
IN/PA — 369

METHOD OF MAKING NANOPARTICLES OF PRECISE ISOTOPIC COMPOSITION BY RAPID ISOTOPIC EXCHANGE

ABSTRACT

The present invention relates toamethod of making ligand protected nanoparticles of metal clusters of precise isotopic composition by rapid and spontaneous isotopic exchange,wherein the isotopically pure clusters are $^{107}Ag_{25}(DMBT)_{18}$ and $^{109}Ag_{25}(DMBT)_{18}$. The rapid exchange of the isotopes of the metal atoms helps to understand the mechanisms of the spontaneous structural changes in the clusters.

METHOD OF MAKING NANOPARTICLES OF PRECISE ISOTOPIC COMPOSITION BY RAPID ISOTOPIC EXCHANGE

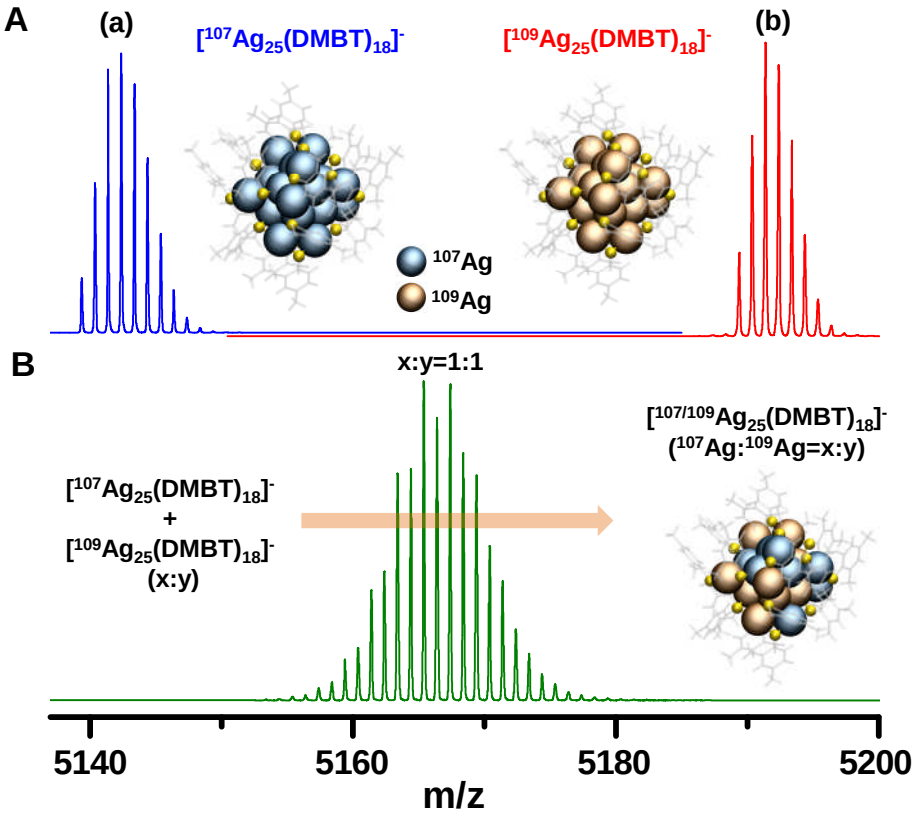

FIGURE 1

Signature:

D. Moses Jeyakaran
Advocate & Patent Agent
IN/PA — 369

METHOD OF MAKING NANOPARTICLES OF PRECISE ISOTOPIC COMPOSITION BY RAPID ISOTOPIC EXCHANGE

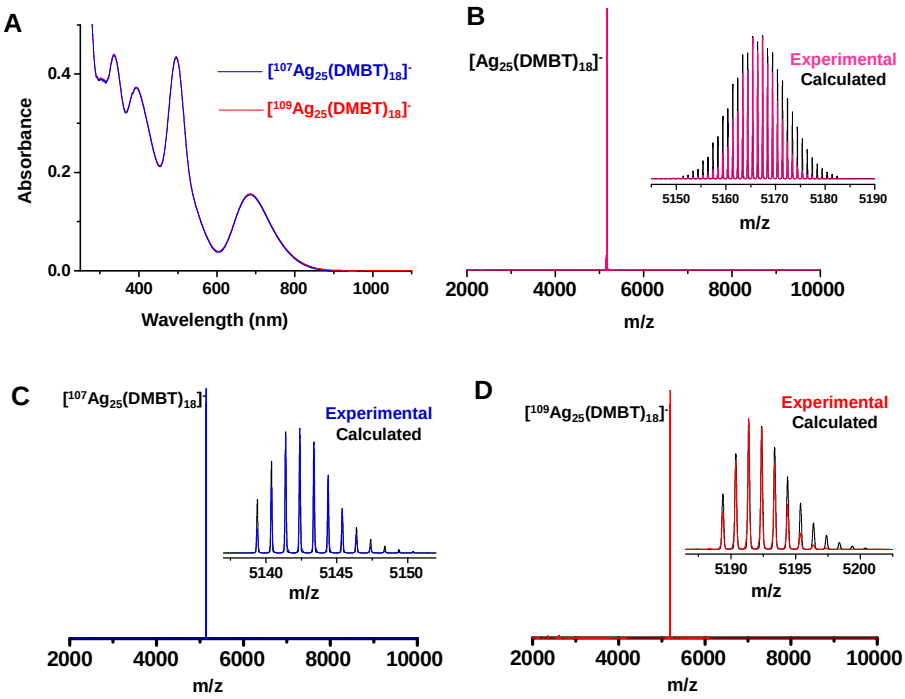

FIGURE 2

Signature:

D. Moses Jeyakaran
Advocate & Patent Agent
IN/PA — 369

METHOD OF MAKING NANOPARTICLES OF PRECISE ISOTOPIC COMPOSITION BY RAPID ISOTOPIC EXCHANGE

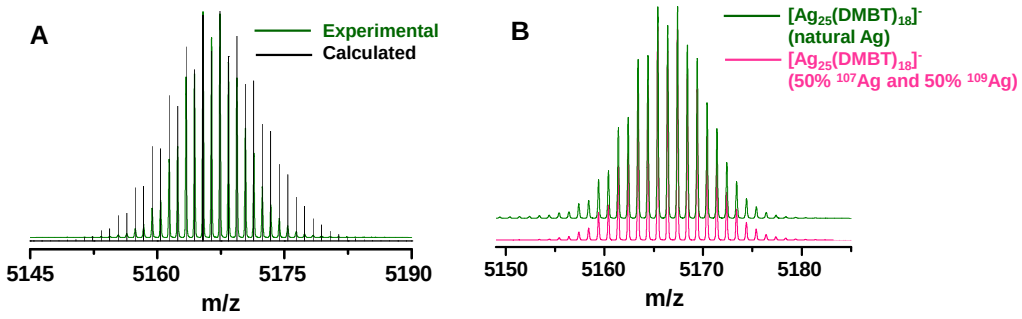

FIGURE 3

Signature:

D. Moses Jeyakaran
Advocate & Patent Agent
IN/PA — 369

METHOD OF MAKING NANOPARTICLES OF PRECISE ISOTOPIC COMPOSITION BY RAPID ISOTOPIC EXCHANGE

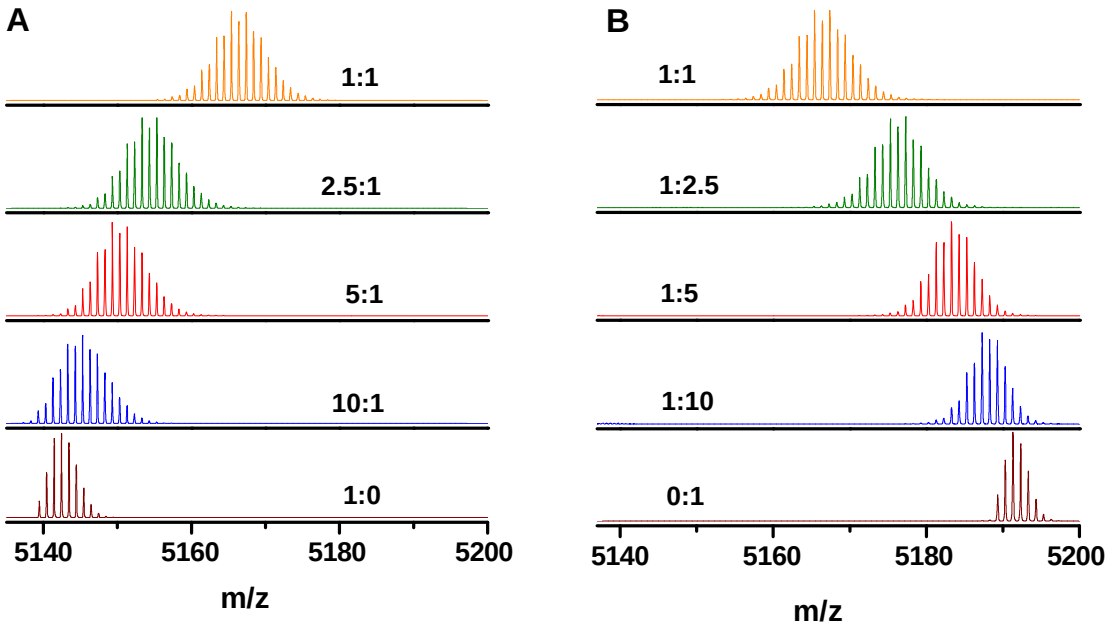

FIGURE 4

Signature:

D. Moses Jeyakaran
Advocate & Patent Agent
IN/PA — 369

METHOD OF MAKING NANOPARTICLES OF PRECISE ISOTOPIC COMPOSITION BY RAPID ISOTOPIC EXCHANGE

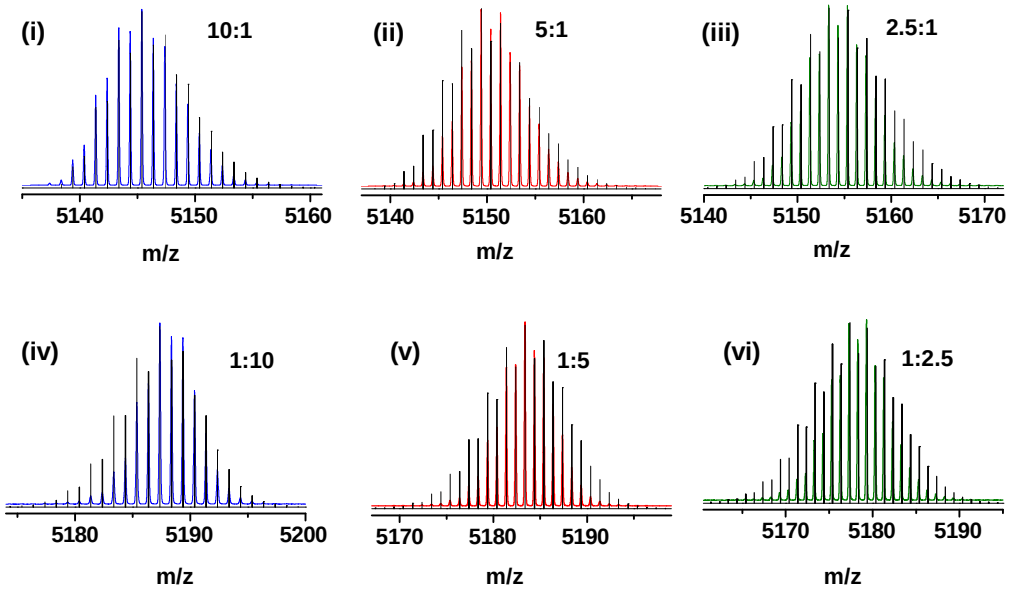

FIGURE 5

Signature:

D. Moses Jeyakaran
Advocate & Patent Agent
IN/PA — 369

METHOD OF MAKING NANOPARTICLES OF PRECISE ISOTOPIC COMPOSITION BY RAPID ISOTOPIC EXCHANGE

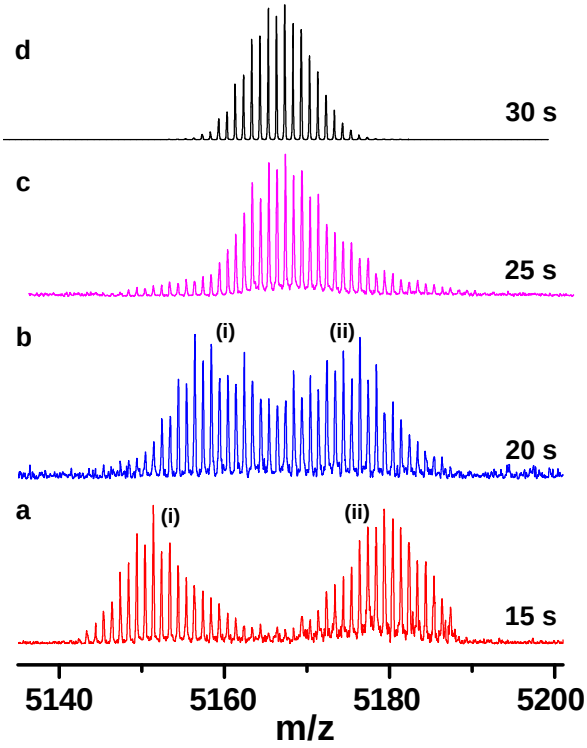

FIGURE 6

Signature:

D. Moses Jeyakaran
Advocate & Patent Agent
IN/PA — 369

METHOD OF MAKING NANOPARTICLES OF PRECISE ISOTOPIC COMPOSITION BY RAPID ISOTOPIC EXCHANGE

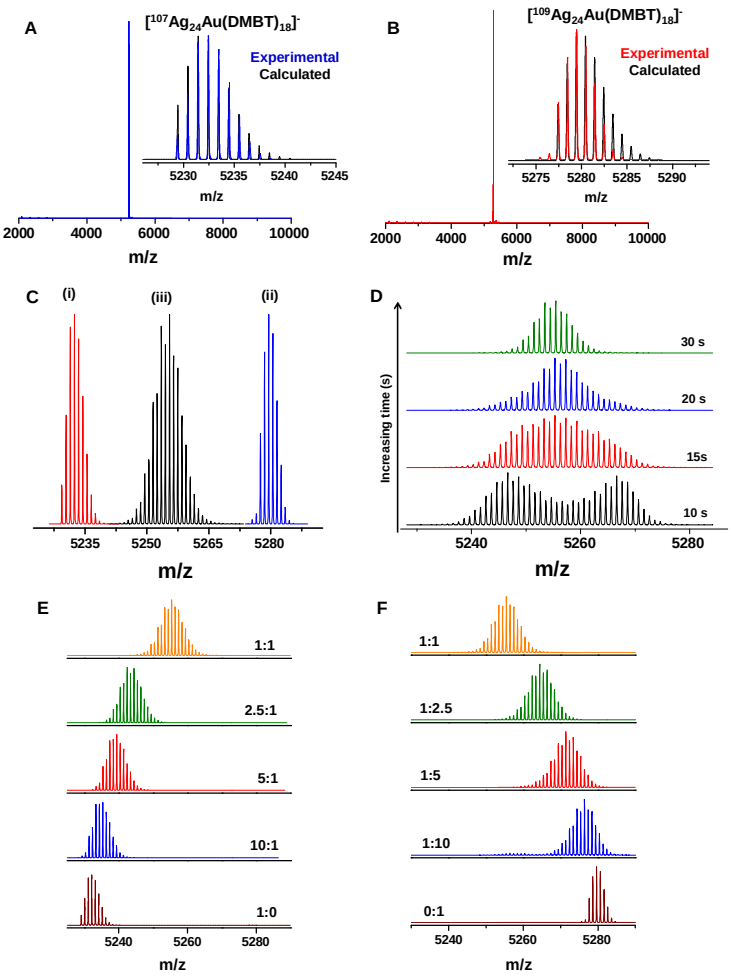

FIGURE 7

Signature:

D. Moses Jeyakaran
Advocate & Patent Agent
IN/PA — 369

METHOD OF MAKING NANOPARTICLES OF PRECISE ISOTOPIC COMPOSITION BY RAPID ISOTOPIC EXCHANGE

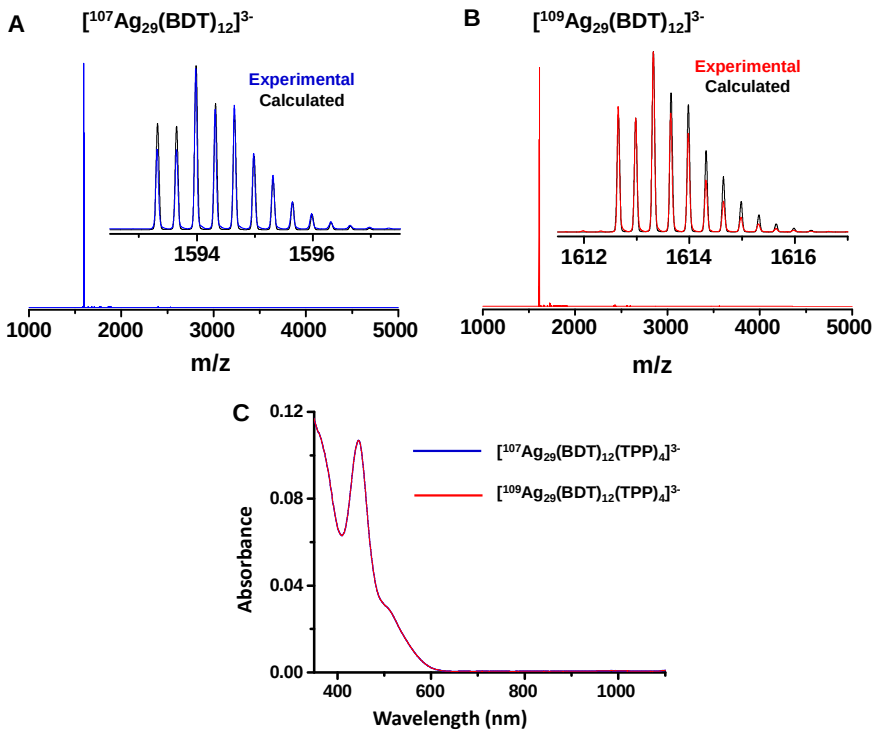

FIGURE 8

Signature:

D. Moses Jeyakaran
Advocate & Patent Agent
IN/PA — 369

METHOD OF MAKING NANOPARTICLES OF PRECISE ISOTOPIC COMPOSITION BY RAPID ISOTOPIC EXCHANGE

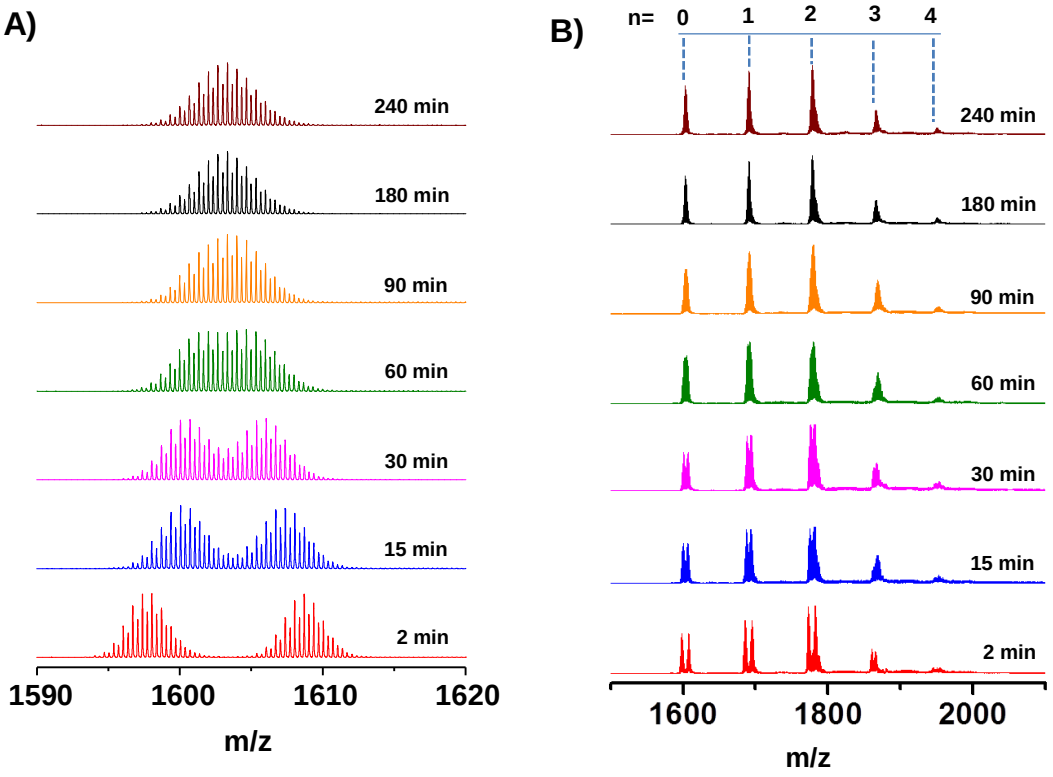

FIGURE 9

Signature:

D. Moses Jeyakaran
Advocate & Patent Agent
IN/PA — 369

METHOD OF MAKING NANOPARTICLES OF PRECISE ISOTOPIC COMPOSITION BY RAPID ISOTOPIC EXCHANGE

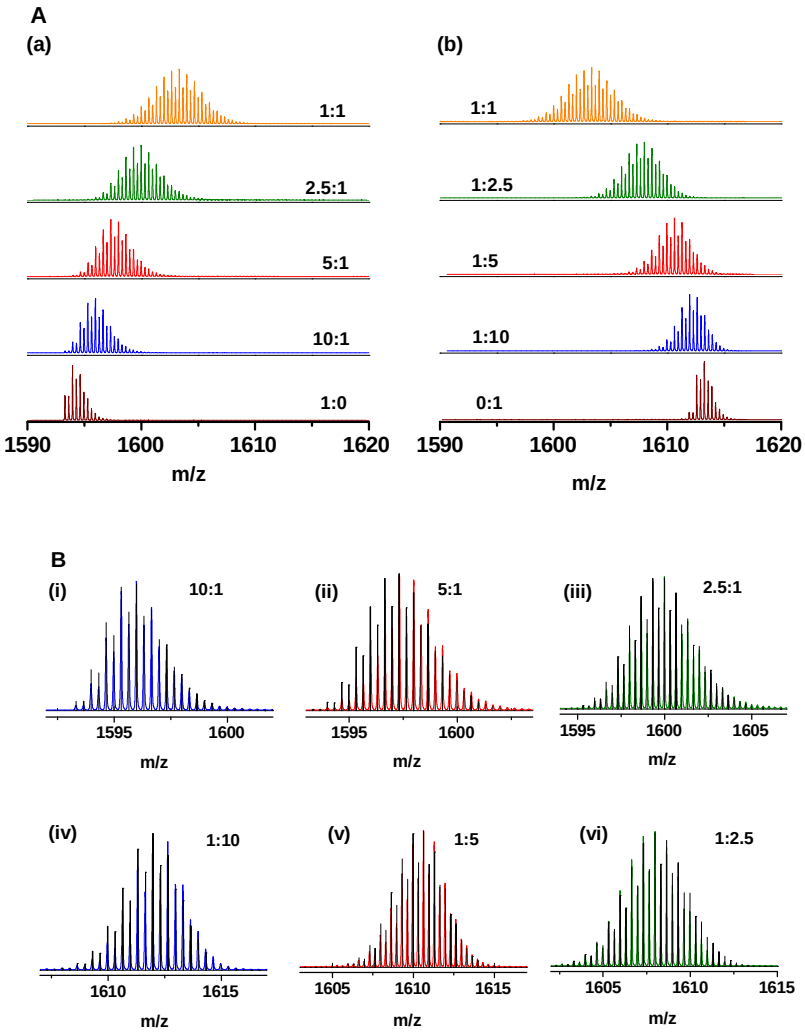

FIGURE 10

Signature:

D. Moses Jeyakaran
Advocate & Patent Agent
IN/PA — 369

METHOD OF MAKING NANOPARTICLES OF PRECISE ISOTOPIC COMPOSITION BY RAPID ISOTOPIC EXCHANGE

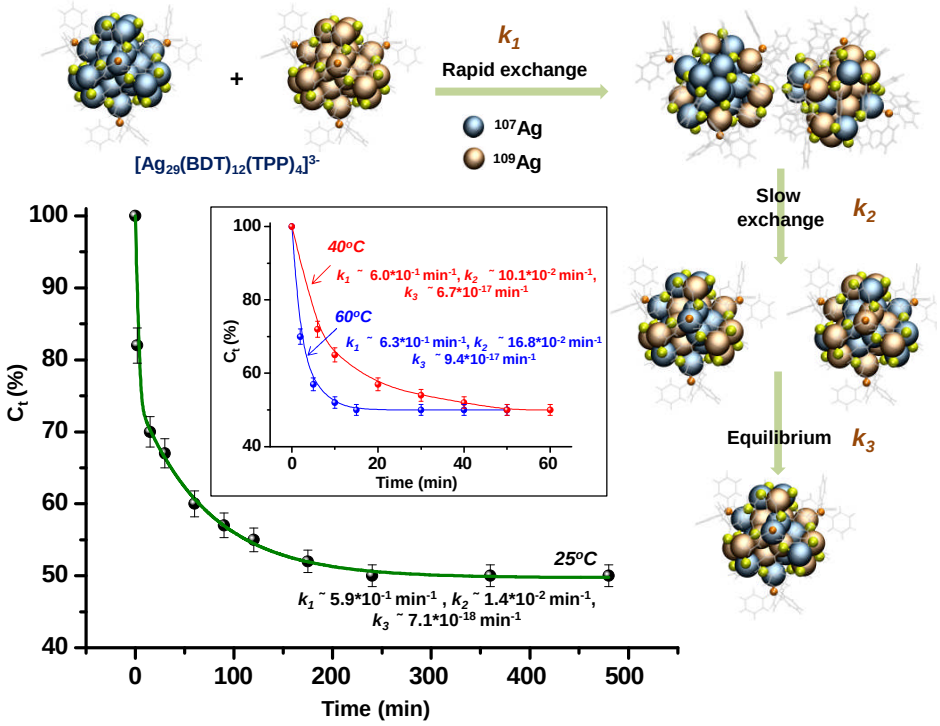

FIGURE 11

Signature:

D. Moses Jeyakaran
Advocate & Patent Agent
IN/PA — 369

METHOD OF MAKING NANOPARTICLES OF PRECISE ISOTOPIC COMPOSITION BY RAPID ISOTOPIC EXCHANGE

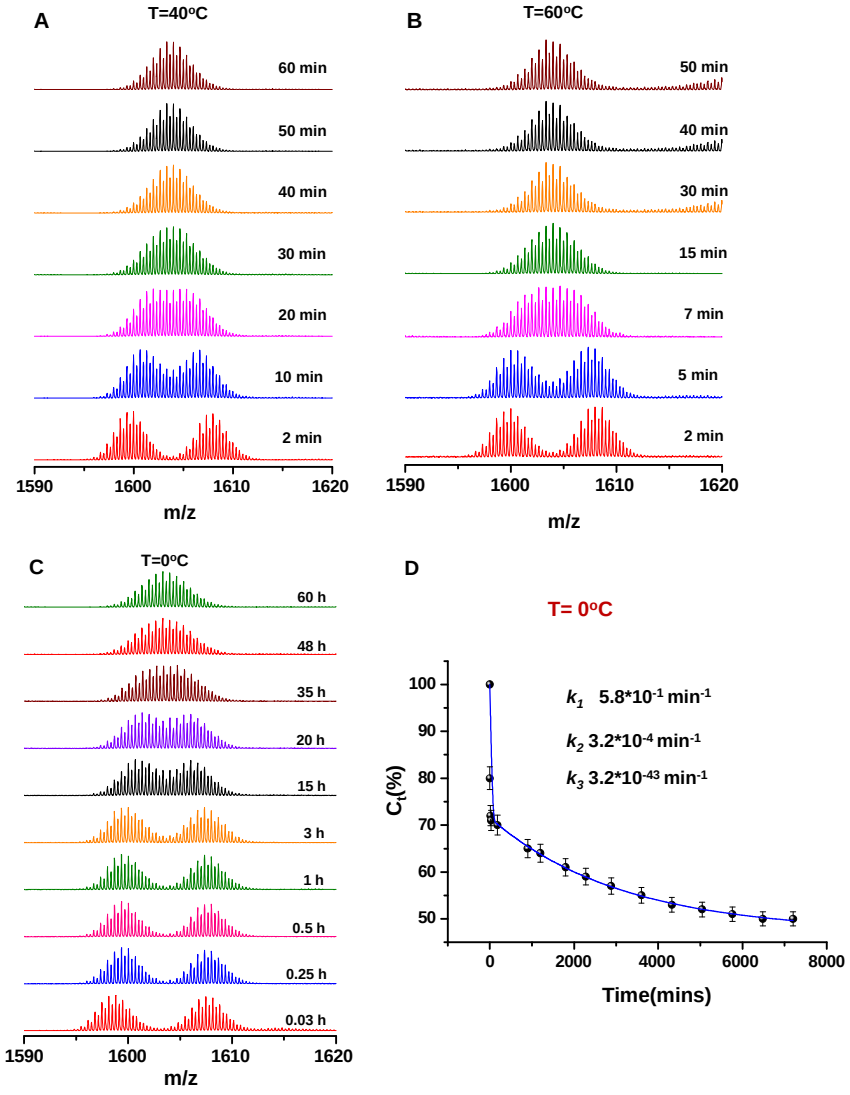

FIGURE 12

Signature:

D. Moses Jeyakaran
Advocate & Patent Agent
IN/PA — 369

METHOD OF MAKING NANOPARTICLES OF PRECISE ISOTOPIC COMPOSITION BY RAPID ISOTOPIC EXCHANGE

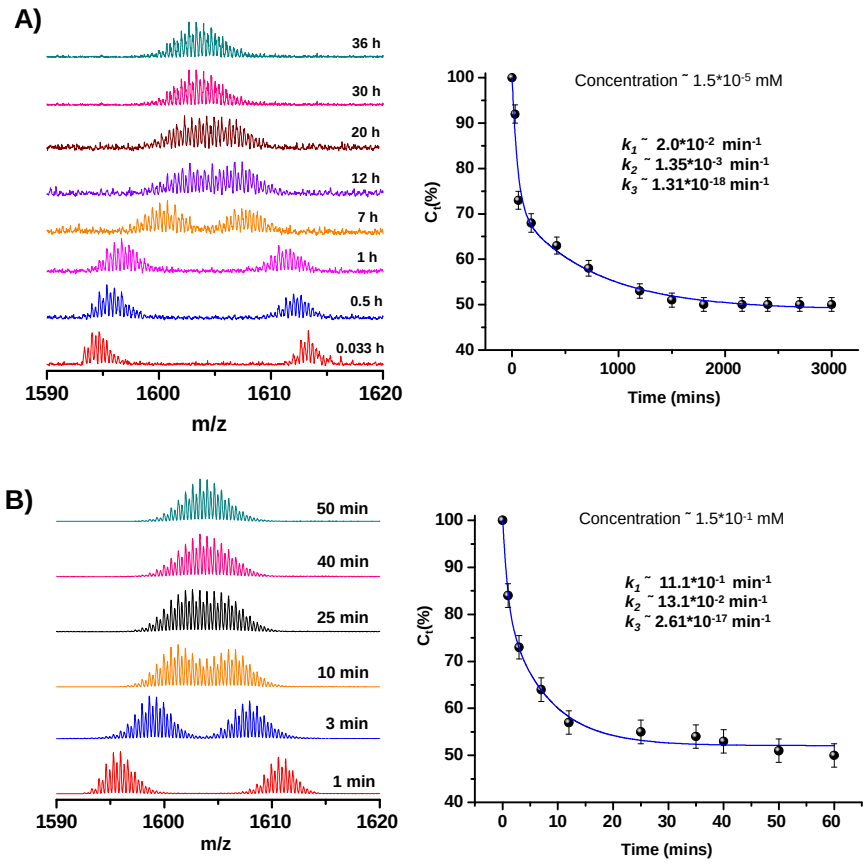

FIGURE 13

Signature:

D. Moses Jeyakaran
Advocate & Patent Agent
IN/PA — 369

METHOD OF MAKING NANOPARTICLES OF PRECISE ISOTOPIC COMPOSITION BY RAPID ISOTOPIC EXCHANGE

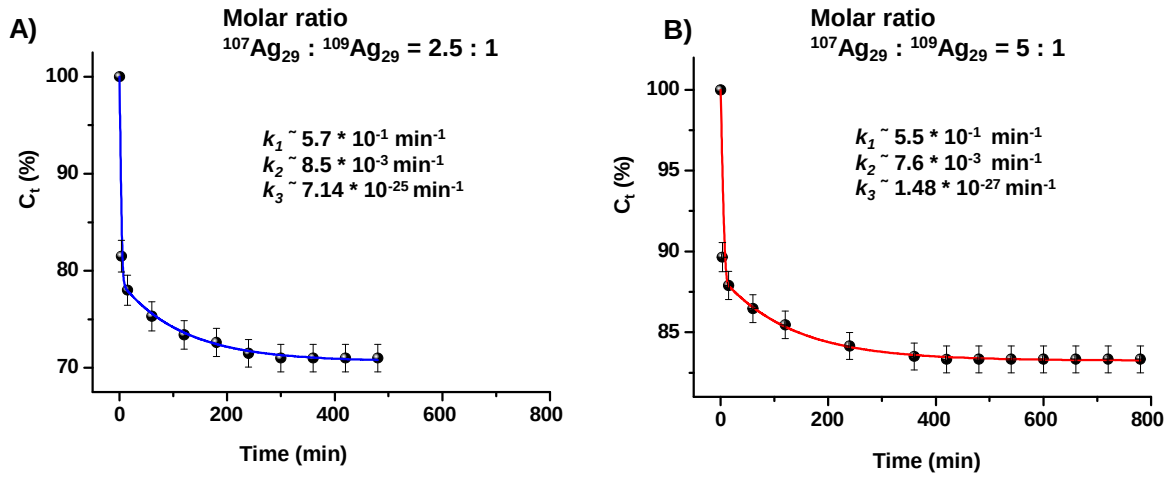

FIGURE 14

Signature:

D. Moses Jeyakaran
Advocate & Patent Agent
IN/PA — 369

METHOD OF MAKING NANOPARTICLES OF PRECISE ISOTOPIC COMPOSITION BY RAPID ISOTOPIC EXCHANGE

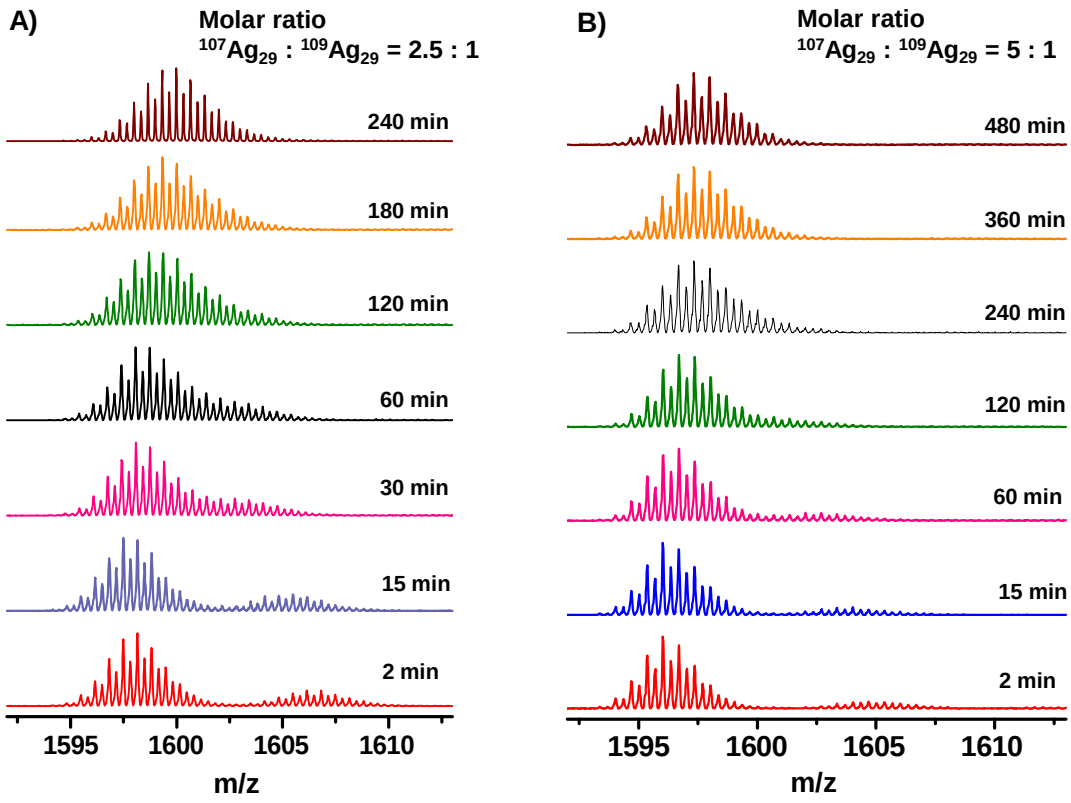

FIGURE 15

Signature:

D. Moses Jeyakaran
Advocate & Patent Agent
IN/PA — 369

METHOD OF MAKING NANOPARTICLES OF PRECISE ISOTOPIC COMPOSITION BY RAPID ISOTOPIC EXCHANGE

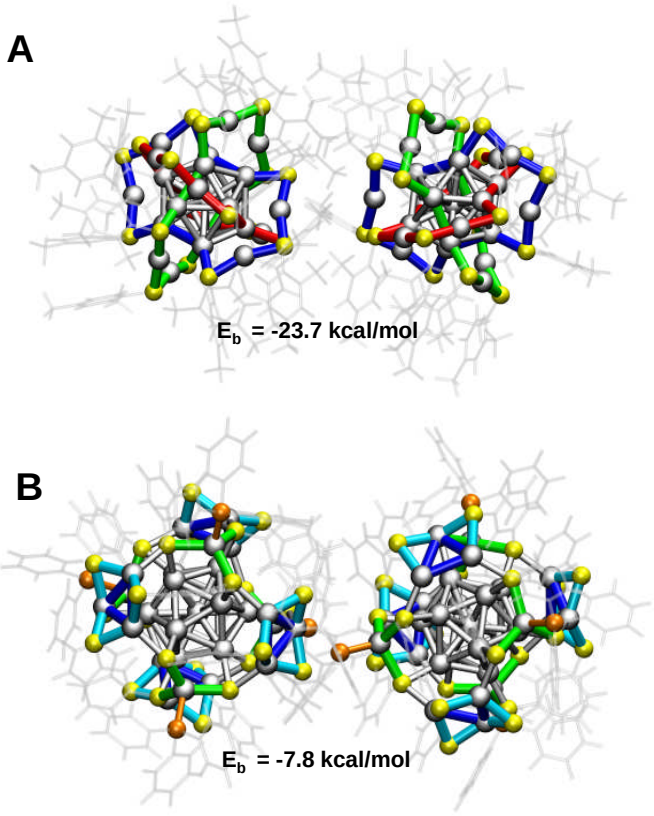

FIGURE 16

Signature:

D. Moses Jeyakaran
Advocate & Patent Agent
IN/PA — 369

METHOD OF MAKING NANOPARTICLES OF PRECISE ISOTOPIC COMPOSITION BY RAPID ISOTOPIC EXCHANGE

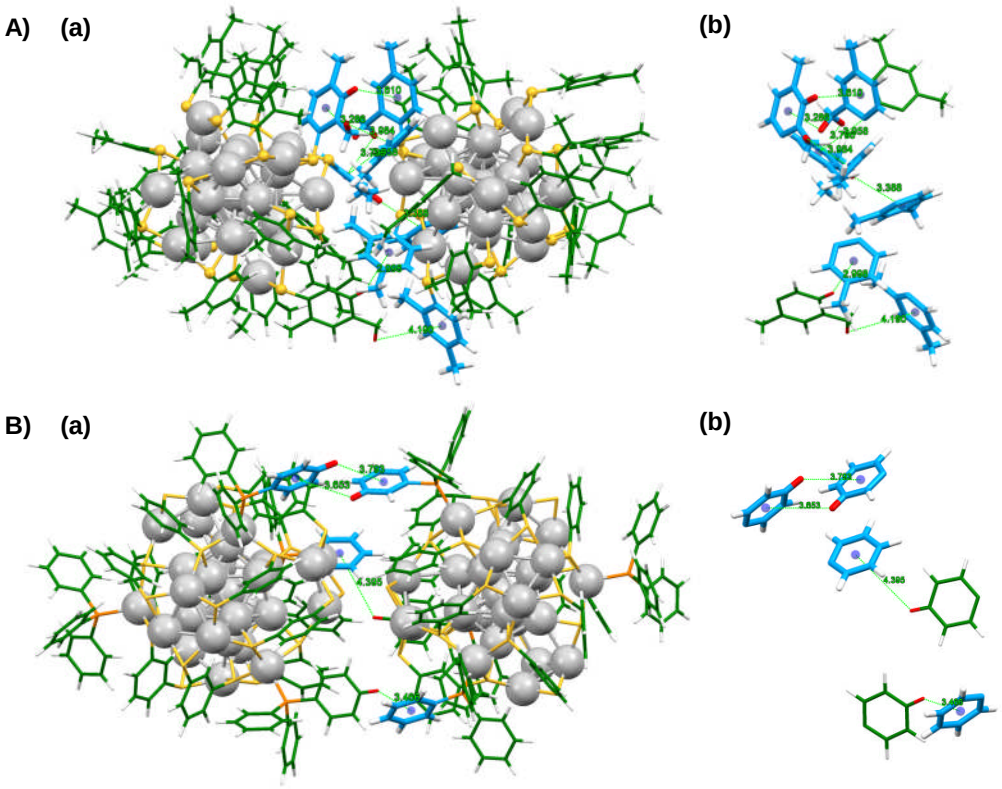

FIGURE 17

Signature:

D. Moses Jeyakaran
Advocate & Patent Agent
IN/PA — 369